Published in final edited form as:
Small. 2016 April ; 12(15): 1968–1992. doi:10.1002/smll.201503396.

Fluorescent Polymer Nanoparticles Based on Dyes: Seeking Brighter Tools for Bioimaging

Andreas Reisch and **Andrey S. Klymchenko***
Laboratoire de Biophotonique et Pharmacologie, UMR 7213 CNRS, Université de Strasbourg, Faculté de Pharmacie, 74, Route du Rhin, 67401 ILLKIRCH Cedex, France

Abstract

Speed, resolution and sensitivity of today's fluorescence bioimaging can be drastically improved by fluorescent nanoparticles (NPs) that are many-fold brighter than organic dyes and fluorescent proteins. While the field is currently dominated by inorganic NPs, notably quantum dots (QDs), fluorescent polymer NPs encapsulating large quantities of dyes (dye-loaded NPs) have emerged recently as attractive alternative. These new nanomaterials, inspired from the fields of polymeric drug delivery vehicles and advanced fluorophores, can combine superior brightness with biodegradability and low toxicity. Here, we describe the strategies for synthesis of dye-loaded polymer NPs by emulsion polymerization and assembly of pre-formed polymers. Superior brightness requires strong dye loading without aggregation caused quenching (ACQ). Only recently several strategies of dye design were proposed to overcome ACQ in polymer NPs: aggregation induced emission (AIE), dye modification with bulky side groups and use of bulky hydrophobic counterions. The resulting NPs now surpass the brightness of QDs by ~10-fold for comparable size and start reaching the level of the brightest conjugated polymer NPs. Other properties, notably photostability, color, blinking as well as particle size and surface chemistry are also systematically analyzed. Finally, major and emerging applications of dye-loaded NPs for *in vitro* and *in vivo* imaging are reviewed.

Keywords

polymeric nanoparticles; fluorescent dye-doped nanoparticles; dye assembly in polymer matrix; aggregation caused quenching; optical bioimaging

1 Introduction

Unraveling the mysteries of life, understanding the basis of disease, achieving personalized medicine, all require methods that combine very high specificity and sensitivity. Especially fluorescence based techniques have made dramatic progress in the analysis of complex biological systems and processes.[1] However, harvesting all the promises of today's fluorescence imaging and detection with respect to speed, resolution and sensitivity, requires fluorescent labels that combine very high brightness and high photostability. Indeed, there is a trade-off between spatiotemporal resolution and sensitivity, and both improve with the

*Corresponding author: andrey.klymchenko@unistra.fr, Fax: +33 368 854313. Tel: +33 368 854255.

Europe PMC Funders Author Manuscripts

brightness of the label: the brighter the emitter, *i.e.* the more photons are emitted for a given illumination intensity, the higher the speed for a given detection limit or resolution.[2] Though high photon emission rates could in principle be achieved using high illumination powers, the photostability[3] of the probe and the phototoxicity experienced by biological samples[4] limit the power that can be used and the time over which a probe can be observed.

Fluorescent nanoparticles (NPs) have the potential to overcome the limits of brightness and photostability of fluorescent dye molecules and fluorescent proteins.[5] At the same time their use as fluorescent labels for bioimaging imposes requirements with respect to their size, their biocompatibility, and their surface chemistry for preventing unspecific interactions,[6] and introducing specific binding to their targets.[7] The field of fluorescent NPs is currently dominated by inorganic NPs especially quantum dots (QDs),[8] dye-doped silica NPs,[9] and upconverting NPs.[10] However, they lack flexibility in terms of tuning emitter properties and surface chemistry. For example, the optical properties of QDs are intimately linked to their core structure and this imposes limits with respect to their brightness.[11] Their use in biological media also requires additional shells, increasing the final size of the QDs to 15 – 20 nm.[12] Similar issues arise in the case of upconverting NPs.[10] The lack of biodegradability of all these NPs also raises long-term toxicity issues.

Fluorescent NPs based on soft organic materials open the way to a better control of emission brightness, color(s), size, surface chemistry, etc. through increased flexibility with respect to the choice, combination, and organization of their constituents.[5a, 13] This spurred recently the development of several approaches to synthesize bright organic fluorescent NPs, notably based on direct assembly of small organic dyes into dye nanoparticles[14] and encapsulation of dyes within lipid[15] and polymer[16] particles. Polymer NPs are particularly promising due their remarkable stability in biological environments and well-controlled surface properties. Conjugated polymer NPs, where the polymer directly plays the role of the fluorophore, evolved in the last years very rapidly, providing a number of very exciting examples of ultrasmall NPs with exceptional brightness.[13, 17] However, similarly to inorganic NPs, conjugated polymer NPs are intrinsically not biodegradable and require a specially adapted organic shell for their stabilization. An alternative approach is to encapsulate small emitters such as dyes or lanthanide complexes inside a non-fluorescent nanosized polymer matrix. This approach is highly promising because it can benefit from the use of biocompatible and biodegradable polymers as matrix materials,[18] and the wealth of preparation techniques and information available from the field of drug delivery.[19] On the other hand, advances in the development of organic dyes[20] provide enormous possibilities in tuning spectroscopic properties of these NPs. Luminescent polymer NPs based on encapsulation of lanthanide complexes is also a very promising direction,[21] though it is out of the scope of this review.

The basic principle for achieving high brightness in dye-loaded polymer NPs relies on confining a large number of dyes in a small space (Fig. 1), thus increasing their absorption coefficient (e.g. $\varepsilon > 10^7$ $M^{-1}cm^{-1}$ for 100 dyes with $\varepsilon \geq 10^5$ $M^{-1}cm^{-1}$ each). However, the flat aromatic structure of fluorophores favors aggregation caused quenching (ACQ) at such high loadings, which is further enhanced through fast excitation energy transfer (EET) due to

small inter-fluorophore distances.[9] Together these ACQ effects strongly decrease the quantum yield and limit the brightness of dye-loaded polymer NPs. Only recently several approaches were introduced that allow strongly reducing ACQ in polymer NPs, notably aggregation induced emission (AIE),[16] as well as dye modification with bulky side groups[22] and bulky counterions.[23] These new possibilities together with the increasing need for ultrabright fluorescent probes lead currently to a rapid growth of the field of bright dye-loaded fluorescent polymer NPs. The aim of this review is to introduce this relatively new field, focusing on the examples where large amounts of dyes were loaded into polymer NPs in order to achieve superior brightness. For these particles we chose the term “dye-loaded” polymer NPs to differentiate them from “dye-doped” polymer NPs where organic dyes are encapsulated at low concentrations to avoid ACQ. The latter were nicely reviewed recently with respect to biomedical applications.[24] A pioneering review on fluorescent polymer NPs that highlights the encapsulation of large amount of dyes appeared very recently.[16] It focuses on bright polymer NPs based on AIE dyes and conjugated polymers together with their biological applications. In the present review, we will describe strategies for synthesis of dye-loaded polymer NPs. We will show limitations of conventional dyes inside polymer NPs and focus on different concepts of dye design for high loading with reduced ACQ. Then, each fundamental property of fluorescent NPs, such as brightness, color, photostability, blinking, size, surface chemistry and stability will be analyzed separately for different examples of dye-loaded NPs. Based on this analysis, we will define the strengths and weaknesses of dye-loaded polymer NPs compared to conjugated polymer nanoparticles[17b, 25] and quantum dots,[8a, 26] which are already well-established. Finally, the scope of their application for in vitro and in vivo imaging will be discussed. Here, we tried to combine and analyze a maximum of examples of dye-loaded NPs, though we could not include all of them because of the size limits.

2 Synthesis of dye-loaded polymer NPs

Over the last twenty years various approaches for the synthesis of NPs from various polymers with well-defined sizes, size distributions, and surface chemistries, and with high and efficient loading of small molecules have been established. The reader is refereed to several comprehensive reviews dedicated to synthesis of polymer NPs, [19a, 19b, 27] including those based on AIE dyes.[28] In this chapter, we will briefly present the main synthetic concepts in relation to dye encapsulation. Synthesis of polymer NPs is most-often realized starting either from preformed polymers that are assembled into NPs, or from the corresponding monomers that are polymerized in emulsions to yield NPs.

2.1 Polymerization-based strategies

Polymer NPs can be directly synthesized through polymerization of the monomers in different types of emulsions. Depending on the composition of the system and the used conditions, the course of the polymerization differs, and one distinguishes typically between (conventional) emulsion, mini-emulsion, and micro-emulsion polymerization (Fig. 2 and Table 1).[29]

2.1.1 Conventional emulsion polymerization—In conventional emulsion polymerization monomers of low water solubility are dispersed with a surfactant (typically above critical micelle concentration, cmc) in an aqueous phase, leading to the presence of relatively large monomer droplets (1-100 μm), monomer swollen micelles, and a small amount of dissolved monomer (Fig. 2).[30] Initiation of polymerization is achieved in the aqueous phase leading to nucleation of the monomer swollen micelles. Polymerization then takes place in these nucleated micelles with continuous monomer diffusion from the monomer droplets to the micelles. Typically, sizes in the range of 50 to 300 nm are obtained, which depend on the kinetics of the polymerization. The used surfactant is incorporated on the surface of the particles and stabilizes them. As its removal or even exchange is difficult, surfactant free emulsion polymerizations have been developed, though the typical size of the obtained NPs is > 200 nm.[31]

Dye-loaded fluorescent polymer NPs have been synthesized through emulsion polymerization using notably styrene[22b, 32] and acrylates (mostly methylmethacrylate and hydroxyethylmethacrylate) as monomers.[33] Emulsifier free methods have also been applied,[34] as well as approaches using emulsifier concentrations below the cmc.[35] A co-monomer with two polymerizable bonds, such as divinylbenzene, can be used to obtain crosslinking of the polymer NPs.[36] In emulsion polymerization approaches the dye is most often incorporated during the polymerization in the form of a dye monomer, though physical trapping is also possible.[34a] A limitation of conventional emulsion polymerization, especially at high dye loading, is the fact that polymerization takes place in the micelles and not in the initially dispersed monomer droplets. Both, monomer and dye thus have to diffuse through the aqueous phase, which makes achieving homogeneous dye loading more challenging.

2.1.2 Mini-emulsion polymerization—In mini-emulsion polymerizations, the size of the monomer droplets is strongly reduced by applying high shear forces (high-speed mechanical stirring or sonication), and through addition of a water insoluble costabilizer (e.g. hexadecane).[27b, 43] Initiation can occur either in the aqueous phase or directly in the droplets. The droplets yield then directly the NPs after polymerization, thus encapsulating dyes present initially in the monomer droplets. The concentration of the surfactant is generally kept below the cmc, leading to the absence of micelles and to an incomplete coverage of the NPs. Further stabilization of the NPs is thus necessary. Their sizes depend on surfactant and co-stabilizer concentration as well as on the homogenization, being typically 30 to 200 nm, often smaller than those obtained through emulsion polymerization. Mini-emulsion procedures are also mostly applied to the synthesis of poly(methyl methacrylate) (PMMA) and especially polystyrene (PS) NPs.[38–40, 44] The dyes are encapsulated either through copolymerization[39–40] or physical encapsulation.[38, 44a]

2.1.3 Micro-emulsion polymerization—In micro-emulsion polymerization a thermodynamically stable emulsion of, typically, a monomer phase in an aqueous phase is formed spontaneously and then polymerized.[45] The very small droplets are stabilized with high amounts of surfactants (~10 % for only a few % of monomer). Initiation can occur in the aqueous phase or in the droplets. In general, very small NPs of 5-50 nm can be obtained

through this technique. However, inhomogeneous nucleation of the particles leads to destabilization of the microemulsion, increase in the particle size, and formation of empty micelles. The identity of particles is thus only partially preserved in micro-emulsion polymerizations, which has to be considered in the preparation of dye-loaded NPs. Micro-emulsion polymerization has been mainly used for the synthesis of polystyrene based dye loaded NPs often crosslinked with divinylbenzene. The dyes have been embedded into NPs either during polymerization[46] or after particle formation through swelling procedures.[41] Moreover, covalent linkage to reactive groups inside and on the particle surface has also been performed.[42, 47]

2.2 Strategies based on preformed polymers

Preparation of NPs can be also realized after synthesis of a polymer. In this case a broader scope of polymers can be used, including some biodegradable polymers, such as poly(lactic-*co*-glycolic acid) (PLGA) and polycaprolactone (PCL) and some specially designed block-copolymers. The three main approaches are used to prepare dye-loaded NPs from preformed polymers: emulsion solvent evaporation, nanoprecipitation, and self-assembly (Fig. 3 and Table 2).

2.2.1 Emulsification solvent evaporation—In emulsification solvent evaporation [19a, 48] the polymer is first dissolved in a water immiscible, volatile solvent, most-often dichloromethane or ethyl acetate. This solution is then dispersed in an aqueous phase typically with the help of a stabilizer and using strong shearing (high-speed homogenization or sonication), resulting in an emulsion of droplets of solvent, containing the polymer. The polymer NPs are then formed through evaporation of the solvent and can be purified by ultracentrifugation. The particle size decreases with the amount of stabilizer but depends also on homogenization. Typically NPs of around 200 nm are obtained with this technique, but it is possible to decrease the particle size to less than 100 nm. For dyes not linked to the polymer, the compatibility and solubility of dye and polymer have to be considered to avoid phase separation upon solvent evaporation.[49] Examples in the literature are often based on PLGA or similar polymers, in which the dyes are encapsulated through physical trapping.[49–50]

2.2.2 Nanoprecipitation—In nanoprecipitation, also called solvent displacement, the polymer is dissolved in a water miscible solvent, *e.g.* tetrahydrofuran (THF), dimehtylsulfoxide (DMSO), acetonitrile. Upon addition of this solution to an aqueous phase, rapid diffusion of the solvent into the aqueous phase (and *vice versa*) leads to supersaturation of the polymer and the formation of NPs.[51] Nanoprecipitation is essentially a kinetically controlled process,[52] so that concentration of the polymer, relative amounts of organic and aqueous phase, presence of stabilizers and details of the mixing influence particle size.[51b, 53] Addition of a stabilizer is, however, not mandatory for formation of small NPs. In its absence, polar groups like polyethylene glycol (PEG) or charged groups on the polymer play an important role in the particle formation.[54] NPs from <10 nm to several hundreds of nanometers can be obtained through this technique. The kinetically controlled formation mechanism facilitates entrapment of dyes.[55] However, strong differences in the solubilities of dye and polymer in the organic or/and aqueous phase

Europe PMC Funders Author Manuscripts

can, at high dye loadings, influence particle formation[56] and thus lead to inhomogeneous distribution of the dye within NPs.[49] For example, we observed formation of large particles and even aggregation when using a few percent of a hydrophobic cationic dye with small inorganic counterions.[23]

Nanoprecipitation is probably the most used method to obtain dye-loaded polymer NPs, and various distinct approaches have been developed. The most straightforward approach uses mixtures of dyes and polymers in the organic phase to achieve physical trapping of the dyes in the formed polymer NPs. This approach was notably applied to PLGA NPs using various dyes.[22c, 23, 57] Another approach uses amphiphilic polymers like poly(maleic anhydride-alt-octadec-1-ene)-PEG (C18PMH-PEG)[58] or PEG containing lipids as 1,2-distearoyl-sn-glycero-3-phosphoethanolamine-N-(polyethylene glycol) (DSPE-PEG).[59]. In these cases the polymer or DSPE-PEG are thought to basically coat and stabilize the NP core composed mainly of dyes. Preformed fluorescent polymers can also be used in this technique.[60]

2.2.3 Self-assembly—Certain amphiphilic polymers, especially block copolymers, have the capacity to self-assemble under thermodynamic control into NPs in the form of micelles.[61] Typically, solutions of the polymer (and, if not part of the polymer, the dye) in an organic solvent are mixed with an aqueous phase, though direct dissolution of the solid polymer in an aqueous phase is also possible. When the concentration exceeds cmc, the aggregation of the hydrophobic parts of the polymers takes place with the hydrophilic parts forming a brush-like shell. . As the amphiphilic polymer plays itself the role of the surfactant and stabilizer, additional surfactants are not used Self-assembly allows preparation of very small NPs ranging from <10 nm to about 100 nm.[62] Most often amphiphilic block copolymers, built from hydrophilic blocks of, *e.g.*, PEG or charged polymers like poly((meth)acrylic acid) and hydrophobic blocks of polymers like PS, PMMA, PCL, or PLGA, are used. The particle size depends on the absolute and relative lengths of the blocks.[61a, 63] However, self-assembly is also obtained with some amphiphilic random copolymers, in which case the particle size depends on the relative amounts of hydrophilic and hydrophobic monomers.[64] This strategy can even be applied to the assembly of fluorescent NPs from single polymer chains.[65]

Unlike nanoprecipitation, self-assembly is generally a thermodynamically controlled process, so that the particles are in equilibrium with their constituting polymers dissolved at the cmc. In consequence, self-assembled block copolymer micelles can undergo exchange, and their stability on dilution is questionable.[66] When dyes are encapsulated, such a dynamic equilibrium can also contribute to dye leaching. Therefore, the dyes are often covalently linked to the polymer.[64, 67] Different strategies have thus been introduced to cross-link the core or the shell of the micelles.[62a, 68]

3 Dye design and encapsulation strategies

In dye-loaded polymer NPs, as in NPs for drug delivery, high and efficient loading are important. A major difference between these two types of NPs is that, while in the latter the encapsulated drugs are usually intended to be released from the NP into the environment (e.g. a tumor or the cytosol), the release of dyes from fluorescent polymer NPs is unwanted,

and often also detrimental to their use in bioimaging applications. Indeed, dye leaching decreases the fluorescence brightness of NPs, while increasing the background signal from the released dyes. In consequence, encapsulation should be performed in a way that fixes the dye strongly inside the particle. In general covalent and non-covalent strategies are used. In non-covalent approaches the dye is physically entrapped inside NPs during their preparation or through swelling procedures with preformed NPs. These approaches are simple, but they suffer sometimes from inefficient encapsulation and dye leaching in biological media. Therefore, they require sufficiently apolar dyes that could be efficiently and strongly entrapped within the hydrophobic polymer matrix. Covalent linking of dyes with polymers constituting NPs can resolve the problem of dye leaching. However, it requires introducing reactive or polymerizable groups into the dyes and optimizing reaction or polymerization conditions in order to achieve high dye loading. The second key problem related to high dye loading is aggregation caused quenching. Indeed, while encapsulating ≤0.1 wt% of dyes does not pose any problem, loading >1 wt% of dyes leads to ACQ for most of conventional fluorescent dyes, such as rhodamines,[71] cyanines,[57] Nile Red,[72] etc, which strongly reduces the quantum yield. High brightness of NPs can hence not be achieved simply by increasing the dye loading. Therefore, a special dye design and encapsulation protocols are required to control organization of the dyes inside the polymer matrix with minimal ACQ. Below, we first analyze the behavior of conventional dyes with respect to loading and aggregation and then describe several solutions developed over recent years to achieve high dye content in particles together with high fluorescence quantum yield (QY).

3.1 NPs encapsulating conventional dyes

The simplest approach is to encapsulate conventional (commercially available) dyes into polymer NPs. This can be achieved either by staining already synthesized blank NPs or by encapsulating the dyes directly during the NP preparation. In the first method commercially available NPs can be used that are loaded with conventional dyes using polymer swelling procedures,[73] as it was shown in the case of PMMA[74] or PS[75] NPs (Fig. 4A,B). In this case, the loading efficiency depends directly on the dye hydrophobicity. A very popular example of a hydrophobic dye used for encapsulation is Nile Red.[72, 76] In a detailed study by Resch-Genger and co-workers using the swelling protocol for 100 nm PS NPs, it was found that the optimal loading giving the highest brightness was 0.8 wt%.[75] However, already at this loading the QY (22%) was significantly decreased compared to that at the lowest dye loading (0.05 wt%, 76%). The second approach is encapsulation of dyes during preparation of NPs. Particularly popular are cyanine dyes, because they are well known for their high brightness and spectral range that spans almost all the visible spectrum up to the NIR region. A first important example is the FDA (Food and Drug Administration) approved NIR dye indocyanine green (ICG) that was frequently encapsulated into PLGA NPs.[77] In these cases the dye content in the 100 – 300 nm particles did not exceed 0.2 wt%. Much smaller particles of 30 nm with encapsulated ICG were obtained using the block-copolymer poly((styrene-alt-maleic anhydride)-block-styrene), though the dye loading remained ~0.3 wt%.[78] Law and co-workers used different cyanines bearing long alkyl chains (DID and DIR) at increased loading inside PLGA NPs.[57] Nanoprecipitation of PLGA-PEG block-copolymers together with the dyes led to NPs of 70-90 nm with dye loading between 0.05 and 3 wt%. It was observed that at 0.5 wt% loading the quantum yield was still satisfactory,

namely 21 and 16% for DID and DIR, respectively, while at higher loading rapid drop in QY was observed. As a result the highest particle brightness was achieved at 0.72 wt% of DID dye loading (Fig. 4C). These and later studies also showed that it was possible to encapsulate multiple cyanine dyes to obtain multicolor NPs, which can be of interest for multiplex sensing and imaging applications.[79] Rhodamine 6G, an important laser dye, was encapsulated in poly(methyl methacrylate)-based NPs of various sizes (20-160 nm) prepared by emulsion polymerization.[35] It was shown that for the dye loading in the range from 0.066 to 0.4 wt% the QY remained stable (68-78%), thus showing no sign of self-quenching. However, higher dye loading led to a drastic drop of the quantum yield, clearly due to ACQ. Similar results were obtained for crosslinked polymeric micelles with core diameters of 13 or 19 nm and hydrodynamic diameters of 23 – 25 nm loaded with fluorescein, cypate (a cyanine 7 derivative), or HL 800 that were covalently linked to the polymer.[62a] In the case of fluorescein the QY dropped to less than 9 % for more than 15 dyes per NP, corresponding to a loading of about 0.7 wt%. QYs of more than 20 % could only be achieved at loadings of less than 0.5 wt% corresponding to larger dye-dye distances. The same observations were made for the other dyes. Hydrophobically modified squaraine dyes were encapsulated in 30-40 nm NPs made with the amphiphilic polymer poly(maleic anhydride-alt-octadec-1-ene) (C18PMH).[70] At 0.5 wt% loading the dye showed a quantum yield of 25 %. In another study the laser dye pyrromethene 567 from the BODIPY family was loaded using a swelling procedure into <30 nm styrene/divinylbenzene NPs, prepared by micro-emulsion polymerization. In this case, NPs with dye loading up to 14 mM (~0.5 wt %) and remarkably high quantum yields (81-84 %) were obtained.[41]

Thus, it is clear that conventional dyes were systematically encapsulated inside polymer matrix at dye loading ≤0.5 wt%, because higher dye loading produced ACQ in practically all these dyes families. The main reason for this seems to be the extended pi-conjugation in dyes with flat geometry favoring pi-stacking. Below we will describe several concepts of molecular design that are currently exploited to overcome ACQ in fluorescent NPs.

3.2 Aggregation-induced emission dyes

Since the works on the exciton theory of J- and H-aggregates, it has been known that certain arrangements of dyes may allow efficient fluorescence in the solid state.[80] However, examples of these systems were mainly limited to J-aggregates.[81] In the early 2000s, Tang et al[82] and Park et al[83] provided examples, where molecules unable to fluoresce in solution became fluorescent in the solid state. To achieve this property, dyes usually bear sterically hindered aromatic groups, such as diarylamino and particularly tetraphenylehtylene and/or bear dipolar functionalities. These molecules are frequently quenched in solvents (polar solvents in particular) because of internal rotation produced by, for instance, twisted intramolecular charge transfer (TICT) states with forbidden fluorescence.[84] By contrast, in the solid state, these rotational motions are inhibited, while the bulky groups, arranged like propeller blades, prevent direct pi-stacking or J-aggregation but favor a kind of distorted H-aggregates allowing fluorescence. This phenomenon named “aggregation-induced emission” (AIE), became very popular recently and gave rise to intensive research on new molecules presenting the AIE behavior.[85] Recent works showed that some of these molecules are highly promising for preparing polymer nanoparticles with

very high dye loadings.[16] NPs encapsulating these dyes are often obtained through nanoprecipitation together with an amphiphilic polymer as encapsulating or coating agent. Particularly successful in this respect was the use of the lipid-polyethylene glycol conjugate DSPE-PEG, which enables further NP functionalization.[69a, 86] In a selected example, Tang and co-workers reported 30 nm NPs based on an AIE fluorogen AIE1 coated by DSPE-PEG. These NPs had a quantum yield of 24 % with emission in the far red region (671 nm) and brightness 10-fold higher than commercial Qtracker 655 (Fig. 5).[59a, 87] A similar strategy was used to prepare 37 nm NPs based on fluorogen AIE2 and AIE4, which gave high quantum yields of 55 and 67 %.[69b] A second polymer often used is the amphiphilic C18PMH-PEG. For example, fluorogen AIE3 was first nanoprecipitated giving bare NPs that were further coated with C18PMH-PEG under ultrasonication.[58b] The obtained NPs of 70 nm size showed QY of 14.9%. Using similar strategies, 30 nm NPs based on fluorogen AIE6 were also obtained. These NPs displayed a QY of 58 % with an extinction coefficient ~ 4×10^7 $M^{-1}cm^{-1}$.[87] Although the AIE dye content inside these NPs cannot be easily estimated, it is expected that the particle core is composed of pure dye (Fig. 5), in contrast to conventional dyes highly diluted in the polymer matrix.

Some attempts were also made to encapsulate AIE dyes inside a hydrophobic matrix made of the biodegradable polymer PLGA. In one study, NPs of 177-202 nm size were prepared using the emulsion solvent evaporation method from a mixture of PLGA/PLGA-PEG-folate together with AIE6 dye and different amounts of PVA as emulsifier.[49] It was found that the amount of emulsifier may modify the dye aggregation inside the PLGA matrix. While low PVA content (0.5 %) favored the aggregated state of the dye with relatively high fluorescence quantum yields (30 %), the higher PVA content (2.5 %) produced rather homogeneous dye distribution in the matrix giving 1.8-fold lower quantum yields.

Furthermore, block copolymers, including poly-(ε-caprolactone-*b*-ethylene glycol) (PCL-PEG), poly(styrene-*b*-ethylene glycol) (PS-PEG), and poly(styrene-*b*-methacrylic acid) (PS-PMAA) have been applied to fabricate AIE NPs.[62b] For example, NPs encapsulating the red emissive AIE3 and the green emissive AIE5 dyes have been obtained in this way. The particle sizes varied from 61 to 91 nm depending on the nature of the polymer and the loading of the dye, which was varied from 1 to 40 wt%. Among the reported NPs, the PS-PMAA nanoparticles gave the smallest NPs (61-68 nm) and the highest quantum yields of 62.1% for AIE5 (30 wt%) and 22.3% for AIE3 (5 wt%).

Despite the beauty of the AIE concept and very promising recent results, it has some limitations. The extinction coefficients of the AIE dyes is generally in the range of 10000-30000 $M^{-1}cm^{-1}$, which is 3-10 fold lower than those of conventional dyes, such as rhodamines (100 000 $M^{-1}cm^{-1}$) or cyanines (150 000 - 250000 $M^{-1}cm^{-1}$). Moreover, their excitation wavelength does not exceed 550 nm for the best recent examples, while in vivo imaging applications would largely benefit from excitation wavelengths in the far red/NIR region (630-800 nm). We expect that a lot of research will be dedicated in the next years to overcoming these limitations of AIE dyes.

3.3 Dyes with bulky side groups

A basic approach to avoid aggregation is covalent modification of dyes with bulky groups that are thought to prevent pi-stacking. One early example deals with a BODIPY derivative (Mes-BODIPY), where a phenyl ring bearing two ortho-methyl groups is nearly perpendicular to the plane of the main fluorophore (Fig. 6). It was encapsulated into 16 nm PS NPs obtained by micro-emulsion polymerization in the presence of divinylbenzene as cross-linker. In this case, high dye loadings of around 3 wt% (76 dyes per NP) were achieved together with remarkably high QY of 77%,[22a] which pointed out the importance of bulky groups to prevent ACQ in dye-loaded NPs. A particularly challenging example in this respect is perylene diimide, which is an important candidate for encapsulation as it is considered to be one of the most photostable dyes to date.[88] At the same time, due to their large flat aromatic system, these dyes tend to form very strong pi-stacked H-aggregates with poor emission. Therefore, significant efforts were made to prevent this process by adding bulky groups at their imide and bay (aromatic rings) regions.[88c] The typical examples are perylene diimide derivatives PDI-1 and Lumogen Red (LR) (Fig. 6). Due to minimized aggregation, they present fluorescence quantum yields close to unity[89] and LR was shown to present minimal self-quenching in PMMA polymer films.[90] However, examples of polymer NPs encapsulating these dyes were lacking or were restricted to very low dye loading (<0.1 wt%).[38] Recently, we studied encapsulation of PDI-1 and LR inside PLGA NPs of 40 nm size.[22c] An increase in the PDI-1 dye loading from 0.02 to 1 wt% produced a drastic modulation of the absorption spectra showing strong aggregation, which was accompanied by the appearance of a new red emission band and a decrease in the quantum yield from 67 to 31 %. By sharp contrast, LR showed weak aggregation for loadings from 0.02 to 5 wt% with the quantum yield varying only from 97 to 47 %. The high LR dye loading and quantum yield enabled preparation of ultra-bright and highly photostable NPs which were ~10-fold brighter than QDs-585, thus showing the benefit of chemical modifications that makes these dyes less flat.

3.4 Dyes with bulky counterions

Paradoxically, the best organic dyes developed to date are the most difficult to encapsulate inside polymer matrices at high loading, so that the examples of NPs with efficient fluorescence are limited to dye loading below 0.5 wt% (see above). The problem is that in addition to a large flat pi-electronic conjugation, the most famous dyes, such as rhodamines and cyanines present a net positive charge. This can both complicate dye loading due to increasing hydrophilicity and facilitate dye aggregation inside the polymer matrix due to the presence of small inorganic counterions. We hypothesized that bulky hydrophobic counterions could serve as isolator of dyes inside the polymer NPs. Previous works of Yao et al[91] and Warner et al[92] showed that bulky hydrophobic counterions, such as tetraphenyl borate and its fluorinated analogues, bis(2-ethylhexyl)sulfosuccinate (AOT), bis(trifluoromethanesulfonyl)imide, etc could decrease the self-quenching of these dyes in the solid state. To validate this concept for polymer NPs, we synthesized a series of salts of cationic rhodamine B bearing a hydrophobic chain (R18) with different hydrophobic counterions that differ in the level of fluorination (Fig. 7).[23] Remarkably, all hydrophobic counterions enabled preparation of very small dye-doped PLGA NPs of ~40 nm size by nanoprecipitation. In contrast, R18 with an inorganic counterion (perchlorate) resulted in

very large PLGA NPs probably because it modified the NP surface leading to aggregation. Importantly, the most fluorinated counterion showed the strongest ability to prevent self-quenching. The obtained 40 nm PLGA NPs encapsulating 5 wt% of the dye displayed a QY of 23 % being ~6-fold brighter than QDs-605. Moreover, single particle microscopy revealed that NPs could undergo nearly complete ON/OFF switching (blinking), suggesting that the bulky counterion not only plays the role of isolator of dyes inside polymer but also ensures sufficiently close proximity of the dyes required for collective behavior of dyes. Later on, the same rhodamine salt was encapsulated at 5 wt% into 20 nm PMMA-based NPs showing QY values of 60% and a single particle brightness about 10 times higher than QDs585.[54b] The application of this approach for cyanines remains to be validated. Nevertheless, we recently showed that this concept works very well for loading of lipid based nanoparticles with up to 8 wt% of a Cy3 (DiI) salt with tetraphenyl borate counterion without significant self-quenching.[15b] We consider that the use of bulky counterions can become a universal concept that enables both efficient encapsulation of conventional charged dyes into the polymer matrix and strong decrease of their self-quenching. It is complementary to the AIE approach, which mainly deals with non-conventional and generally non-charged dyes.

3.5 Dyes with polymerizable/reactive groups

Covalent linking of the dyes to the polymer of NPs has the key advantage of complete absence of leakage in biological environments, which can be the case in the physically encapsulated NPs.[16, 24, 72] In particular many polymerizable dye monomers have been prepared to incorporate the dyes into the polymers through co-polymerization and some of them were introduced inside polymer NPs.[93] Alternatively, the reactive dye could label the already synthesized polymer[94] or NPs[62a, 68a] bearing reactive groups. However, as in the case of physical encapsulation of conventional dyes into polymers, minimal amounts of dyes were used to avoid self-quenching.[33, 34b] To prevent aggregation of PDI derivatives after polymerization Li and co-workers used a twisted derivative bearing four chlorines at the bay region (Fig. 8A).[22b] Thus, using modified emulsion polymerization method, these twisted PDI monomers were covalently embedded within the hydrophobic cavities of polymer NPs based on acrylamide and styrene with minor amounts of functional monomers. The loading of PDI dyes up to 2.4 wt% yielded NPs of 40 nm size with QY of ~50%. Their single particle brightness after 8 min of direct illumination under microscope remained ~50-fold higher than the single monomer dye. Some studies are also available for PDI derivatives without modifications in the bay region. Thus, Wurthner et al developed wedge shaped amphiphiles of perylene-diimide, which assembled into very small micellar NPs of 4-6 nm that were further stabilized by *in situ* polymerization (Fig. 8B).[95] The assembly observed in water/THF mixtures was accompanied by a characteristic change in the color from green emission of the monomer to a significantly weaker red emission of the excimer. Another group used a RAFT-based polymerization approach to obtain a block-co-polymer of perylene diimide acrylate and poly(ethyleneglycol)methacrylate that bears a flat PDI derivative.[67a] This polymer assembled into NPs of 64 nm size and exhibited the red emission characteristic for the PDI excimer. These examples together with our recent data using non-covalent doping of PDI dyes into NPs[15b] show how the twisting of PDI core can drastically change its behavior inside polymer NPs. Recently, Clavier et al using RAFT mini-emulsion polymerization of different BODIPY monomers obtained NPs of 60-90 nm

size containing up to 5000 dyes per particle (Fig. 8C).[96] Despite the high dye loading (3 dyes per polymer chain of 15-20 kDa, ~8 wt% dye loading), QY remained relatively high (35%). Theoretical calculation of brightness suggested that they are 200-2000 times brighter than usual quantum dots. Later works showed the brightness can be further improved by increasing dye loading from 500 to 5000 dyes per NPs, though, in this case, their QY of BODIPY decreased ~3-fold due to ACQ.[97]

An important approach is to utilize AIE fluorophores for covalent encapsulation into polymer NPs.[28] Thus, Wei and co-workers reported cross-linkable AIE fluorophores that were used for preparation of NPs by RAFT polymerization.[98] The obtained NPs had sizes of 280 and 130 nm for degrees of polymerization of the PEG bearing monomer of 20 and 40, respectively. The fluorescence intensity was comparable to that of the polymer in methanol, thought the QY values and the single particle brightness were not described. The same group also synthesized NPs through emulsion polymerization using a monomer based on the same AIE motif.[32a] In another example, amphiphilic block copolymers based on tetraphenylethene, copolymerized by ring-opening metathesis, were assembled into micellar NPs of 25 nm size with a QY of 20 %.[99] Tian and co-workers synthesized amphiphilic polymers bearing AIE dyes as well as methacrylate monomers bearing ammonium, hydroxyl and trifluoroethyl group.[64a] The obtained NPs were very small (7-9 nm) in the case of polymer without trifluoroethyl group, while with the latter group the size increased to 21-25 nm. Remarkably, their QY increased in the presence of trifluoroethyl up to 40 % for 1 mol% of the AIE dye, which was explained by a more compact aggregation of AIE dye in the NPs core.

4 Control of NP properties

When organic dyes are organized in form of NPs, they should present a number of properties that are critically different from those of the single dyes. Firstly, *size* of NPs is significantly larger, which can be a weak point for certain applications that require minimal perturbation of a biological molecule or process, but can be a strong point for *in vivo* imaging and some single particle tracking studies. *Brightness* of NPs can be >100-fold higher than that of single molecules, which can be a great point for numerous imaging applications. *Photostability* is probably one of the most unclear points for dye-based NPs. On one hand encapsulation should improve photostability due to the shielding through the rigid polymer matrix, but dye aggregation may stimulate photochemical process and thus decrease drastically the dye stability. The *color* of NPs is directly defined by the color of encapsulated dyes, though in some cases dye aggregation can generate NPs with different absorption and emission maxima. Moreover, multiple excitation/emission colors can be achieved by co-encapsulation of different dyes. Dyes confined inside a polymer matrix at high concentrations may produce cooperative phenomena, such as particle *blinking*/*switching*. The important feature of NPs is rich *surface chemistry*, which allows grafting of different ligands in multiple copies as well as fine tuning of NPs colloidal stability and surface interactions with biological media.

4.1 Size

Size is a key property of NPs that define their further biological applications. So far, dye-loaded polymer NPs were developed with sizes ranging between 15 and 500 nm. In principle, there is no upper size limitation for polymer NPs, because the fluorescence efficiency of encapsulated dyes does not directly depend on NPs size, but mostly on dye concentration and possible ACQ. In this respect, dye-based polymer NPs have an advantage over inorganic QDs and conjugated polymer NPs, whose size cannot be varied so much. Indeed the size of the semiconductor core of quantum dots varies only between 3-8 nm, while with shells their size ranges between 20-30 nm.[8a, 100] In this case variations of the size of the quantum dot core are also directly linked to changes of the optical properties (e.g. position of the absorption and emission maxima). In the case of conjugated polymer NPs, highly emissive NPs were mainly reported for particle sizes of 10 to 20 nm, with only few exceptions of larger NPs.[17b, 25] It is possible that for larger sizes the quenching phenomena play a crucial role, though this point is not clearly addressed in literature.

A number of approaches were proposed to control the particle size in dye-loaded polymer NPs. In emulsion polymerizations the particle size can notably be controlled through the oil to water ratio, the surfactant type and concentrations, and the homogenization techniques.[29] In this way NPs with sizes ranging from 15 to 500 nm can be obtained with often a very narrow size distribution. The largest particles are usually obtained by emulsifier free and conventional emulsion polymerizations.[31] Mini-emulsion polymerization yields typically smaller NPs in the range 50 to 250 nm.[27b] Still smaller dye based NPs reaching down to 15 nm and less can be obtained through micro-emulsion at the expense of high surfactant concentrations.[45] Approaches based on the self-assembly of polymers can also provide some level of control. Amphiphilic block copolymers bearing hydrophobic and hydrophilic segments have been used for the assembly of dye-loaded polymeric micelles with sizes between 10 and 100 nm,[62] which can be controlled by the overall and relative size of the hydrophobic and hydrophilic segments.[61a, 63, 101] Random amphiphilic copolymers can even give smaller NPs reaching down to single chain NPs.[64–65] A great variety of NPs with AIE dyes was synthesized through nanoprecipitation procedures using the lipid-polymer conjugate DSPE-PEG as stabilizer, which generally resulted in sizes around 30-40 nm.[16] It should be noted that in the case of the most common polymers for biomedical applications such as PLGA, PCL and PMMA, the standard protocols based on nanoprecipitation or emulsification-solvent evaporation give relatively large NPs of 50-300 nm.[19a, 19b, 102] Recently, we proposed an alternative self-assembly approach, which is based on charge-controlled nanoprecipitation. In this case, a single charged group on the polymer, such as PLGA, PCL and PMMA could decrease the size of obtained particles to less than 15 nm.[23, 54b] Thus, by varying a single group at the end of the polymer and the concentration of the polymer in the organic phase it became possible to tune the particle size between 15 and 100 nm.[54b]

4.2 Brightness

The brightness of a fluorescent dye, defined as product of extinction coefficient and quantum yield (ε×QY),[20] determines the signal that can be obtained from a single molecule and thus defines sensitivity and resolution. The extinction coefficient for dye-loaded polymer

NPs depends directly on the number of encapsulated fluorescent dyes. Therefore, to increase the brightness one can increase the dye concentration in the polymer matrix and/or the particle size. For comparison, the brightness of single dyes is of the order of their extinction coefficient, e.g. for rhodamine 101, frequently used as standard for QY measurements[103], $\varepsilon \times QY = 10^5 \times 0.9 = 0.9 \times 10^5\ M^{-1}cm^{-1}$. On the other hand, AIE-based NPs of 30 nm size were 10-fold brighter than QD-655,[59a] which is supported by their high expected theoretical brightness $\varepsilon \times QY = 4 \times 10^7 \times 0.25 = 10^7\ M^{-1}cm^{-1}$ (Table 3). Encapsulation of Mes-BODIPY into PS NPs using micro-emulsion polymerization was achieved with high dye loading and QY that led to 16 nm particles with a theoretical brightness of $n \times \varepsilon \times QY = 115 \times 5.8 \times 10^4 \times 0.77 = 5 \times 10^6\ M^{-1}cm^{-1}$.[22a] In our studies, we showed that NPs of PLGA of ~40 nm were 6-fold brighter than QD-605, which resulted from >500 encapsulated rhodamine B/F5-TPB dyes, i.e. a theoretical brightness of $n \times \varepsilon \times QY = 500 \times 10^5 \times 0.2 = 10^7\ M^{-1}cm^{-1}$. Later on, we were able to decrease the NP size to 15 nm using a modified PMMA matrix. The resulting NPs were nearly 10-fold brighter than QD-585, with theoretical brightness, $n \times \varepsilon \times QY = 39 \times 10^5 \times 0.6 = 2.3 \times 10^6\ M^{-1}cm^{-1}$.[54b] In the case of NPs prepared by RAFT emulsion polymerization, Clavier et al obtained NPs of 60 nm size with theoretical brightness of $14 \times 10^7\ M^{-1}cm^{-1}$, though their single particle brightness was not verified by microscopy.[96] On the other hand, for many biological applications one looks for the brightest possible particle with the smallest possible size. Therefore, brightness per volume is another important parameter that directly addresses the brightness of a given fluorescent material independently of the particle size. As the nanometer scale is of interest here, we present the brightness per volume for polymer different NPs in units of $M^{-1}cm^{-1}nm^{-3}$ (Table 3). It can be seen that all three mentioned above systems based on AIE, rhodamine B/F5-TPB and BODIPY dyes show relatively close brightness per volume. This is not surprising, because in the case of AIE dyes, the large dye concentration is compensated by the relatively low extinction coefficients of the dyes, while in the case of Rhodamine B/counterion and BODIPY-based NPs, the loading and the fluorescence characteristics of dyes are comparable. We should mention that the theoretical brightness calculated from the extinction coefficient and QY and the real brightness under the microscope will not necessarily match. An interesting example is comparison of two AIE derivatives AIE1 and AIE6, giving similar particle size (30 nm) and extinction coefficients.[79] NPs of dye AIE6 presenting twice as high quantum yield as NPs of AIE1 emitted 80-fold lower total number of photons within a 100 s period. This unexpected result shows how important it is to make measurements of brightness directly under the microscope. The reason is that microscopy uses much higher illumination power (10-1000 W/cm^2) compared to the steady state spectroscopy (~1 mW/cm^2), so that several new factors come into play. First, strong illumination provokes faster photo-degradation and therefore, the number of photons collected for a given period of time may decrease. Second, strong illumination induces triplet saturation, where a non-emissive triplet state is generated for a millisecond time scale.[104] Electron transfer can also take place that also produces long-lived dark species.[105] Therefore, all theoretical estimations of brightness of new fluorescent NPs should be complemented with microscopy measurements with respect to a known reference (e.g. QD, etc). Still, care has to be taken as the results depend on the excitation wavelength and power as well as the integration time.

It is important to compare these examples with conjugated polymers, which are often considered as the brightest fluorescent materials to date. Indeed, it can be seen that all mentioned organic systems are about 2 to 5-fold less bright than the best conjugated polymer (PFBT) NPs reported to date (Table 3). However, it should be noted that performance of conjugated polymer NPs strongly varies with the polymer, so that NPs of other absorption and emission color built from other conjugated polymers (MEH-PPV, PFPV, PFO, PPE, etc) are significantly less bright and close to the brightness observed for dye-loaded systems.[17a] Finally, all these examples of polymer NPs are much brighter than QDs both theoretically and practically under the microscope. First, QDs present limited absorption coefficient, especially in the long-wavelength region (>480 nm) typically used for comparison. Taking a QD-605 with excitation around 530 nm as example yields a brightness of $\varepsilon \times QY = 5.8 \times 10^5 \times 0.55 = 3.2 \times 10^5\ M^{-1}cm^{-1}$ (Table 3). Second, QDs exhibit intermittency of their emission especially under strong illumination of the microscope,[106] which significantly decreases their brightness. Third, the emission rate of QDs is much lower than that of organic dyes and especially compared to conjugated polymers, which is clear from comparison of their fluorescence lifetimes, longest for QDs and shortest for conjugated polymers.[25] The slowest emission rate of QDs is also because they are true single emitters, while most of the other fluorescent NPs can be considered to contain several independent emitters that allow emission in parallel.

4.3 Photostability

When organic dyes are encapsulated into the polymer matrix of NPs, their photostability can be influenced by several independent factors. On one hand, being confined within a rigid polymer matrix confers significantly improved photostability to some dyes, notably due to the protection from oxygen or other chemical species that take part in photo-degradation reactions.[77b, 78, 110] For example, encapsulation of ICG into NPs significantly improved the chemical and photostability of ICG, probably due to the confinement effects.[78, 110] In the case of squaraine type dyes, the encapsulation of the dye into C18PMH NPs drastically improved chemical and photostability.[70] On the other hand, at high concentrations, organic dyes may form ground and excited state aggregates, which may change the photochemistry of dyes and provoke a decrease in the photostability.[22c]

Two types of photostability measurements are usually done: illumination of the bulk sample in a cuvette with a lamp or a laser beam or direct observation of single particles under the microscope. These experiments may give very different results because the excitation power under the microscope can be >1000 times stronger. Here we will focus mainly on the fluorescence microscopy data, as they are the most important for bioimaging applications. Usually, two parameters are used in single molecule microscopy measurements: observation (survival) time for a given laser power and the total number of photons collected.[88a] The latter value gives direct access to the quantum yield of photo-degradation. Generally, organic dyes deliver between 10^5 and 10^6 photons and could be observed for periods of 10 to 100 seconds under the strong illumination required for their imaging (~1 kW/cm^2).[88a] Unfortunately, the data on photostability of NPs is much less systematic and is difficult to compare, as they were performed on different setups using different illumination powers. In the case of dye AIE1, it was shown that photobleaching was observed within the time scale

of 100 s with a relatively large total number of collected photons (4.4×10^7).[87] We also studied photostability of PDI based PLGA NPs at the single particle level.[22c] They showed remarkable stability, as under 50 W/cm^2 laser illumination the LR based NPs preserved >80 % of their emission after 100 s of illumination (Fig. 9). However, the total number of photons before photobleaching was not estimated for this system. We expect that as a single PDI molecule is able to deliver ~10^6 photons,[88a] our NPs should theoretically deliver ~10^8 photons. On the other hand, the other PDI derivative, PDI-1, presenting strong emission in the red region from the aggregate (excimer) showed drastically lower photostability, as for the same 50 W cm^{-2} laser illumination it was bleached within the first 10 seconds (Fig. 9), which is in line with another recent report.[111] This result we found particularly surprising in the view of exceptional photostability of PDI dyes.[88a] It can raise the question whether dye aggregation could increase the probability of photochemical reactions (e.g. formation of reactive radical species, cycloaddition reactions, etc) that lead to poor photostability.

Though the total number of photons collected from dye-based polymer NPs is much larger than for single organic dyes, it is slightly less than that for the best examples of conjugated polymers, PFBT, which was reported to deliver 10^9 photons for 15 nm NPs.[17a] However, all other conjugated polymers showed much lower photon number between 10^6 and 10^8, which are in the same order of magnitude as dye-loaded NPs.[17a] Regarding QDs, some reports showed that the total photon number of CdSe QDs is limited to 10^7,[112] whereas other reports suggest higher values that are supposed to be >100-fold larger than rhodamine 6G (i.e. $>5\times10^7$).[100a]

4.4 Color

The key feature of dye-loaded polymer NPs is the presence of well-defined absorption and emission bands, similarly to the parent dyes. This property is particularly important for multicolor imaging. Indeed, in order to detect independently many different types of NPs, they should be selectively excited and detected. Therefore, the critical parameter for fluorescent NPs is the position and the bandwidth of their absorption and emission bands. Ideally, the excitation range should be available from violet (400 nm) up to NIR (800 nm). The possibility of using any kind of organic dye enables preparation of NPs with almost any possible absorption and emission maximum. Thus, it was shown using a PLGA matrix and a set of cyanine dyes, that the color of NPs could be tuned and, if needed, multi-color emission can be generated (Fig. 10).[79] This multicolor emission, obtained by cascade Förster resonance energy transfer (FRET) inside NPs, enabled multiplex-imaging, where, using a single light source, multiple emission colors could be detected. Another example of multi-color polymer NPs encapsulating Coumarin 153 (C153) and Nile Red should be also mentioned.[113]

The interest in the far red and NIR regions is growing rapidly because in these regions auto-fluorescence is minimal and living tissues are more transparent.[114] Far red and NIR regions can be readily reached using corresponding dyes, especially from the cyanine family (Cy5.5, Cy7, and ICG).[24] However, the situation is different for AIE dyes. Generally, the absorption maximum of the AIE dyes developed so far does not exceed 550 nm, which is a

serious shortcoming that will probably be intensively studied in the coming years. The emission of AIE NPs could be more red shifted with emission maxima reaching the far-red/NIR region (600-700 nm).[16, 115] To further extent emission of AIE NPs to the NIR region, they were doped with NIR dyes as FRET acceptors.[116] It should be noted that the bandwidth of the absorption and emission bands of dye-loaded NPs is generally defined by the intrinsic properties of encapsulated organic dyes. However, aggregation can induce broadening of these bands or formation of new ones. [22c, 81, 85] It is important to note that the absorption and emission bands of AIE dyes are generally broader than those of conventional dyes (such as BODIPY, rhodamines or cyanines). However, this weaknesses are compensated by relatively large stokes shifts, which enhance the signal to nose ratio in their fluorescence imaging applications.[16]

Well-defined absorption and emission bands at almost any desirable wavelength of the optical window are a critical advantage of dye-loaded NPs compared to conjugated polymer NPs and quantum dots. The former are characterized by broad absorption and emission bands, so that in practice, multicolor imaging with for instance three colors is difficult because of cross-talk between the channels produced by these bands. Therefore, attempts were made to improve the sharpness of the emission bands by introducing BODIPY dyes inside conjugated polymer NPs.[117] Regarding QDs, their emission bands are sharp, but only at wavelengths below 655 nm. Moreover, their absorption bands overlap in the short-wavelength region, so that they could be all excited by one light source. Though this can be an advantage for multiplexing detection,[118] it can be a source of cross-talk artifacts for multi-color fluorescence imaging.

A particularly important advantage of dye-loaded NPs over conjugated polymer NPs and QDs is their operation in the NIR region. Indeed, for the moment, no conjugated polymer was developed that is able to absorb light in the far red/NIR region (600-800 nm).[25] Their emission reaches the far-red region, but to introduce NIR emission, these NPs require doping with a NIR dye as a FRET acceptor.[119] On the other hand, NIR QDs, such as QD-800, are commonly used, but their absorbance in the NIR region is relatively weak and their emission is very broad.[119] In this respect, dye-loaded polymer NPs are much more flexible in generating narrow absorption and emission especially in the far-red/NIR regions. However, preparation of bright dye-loaded NIR NPs remains challenging because NIR dyes present stronger tendency to ACQ compared to dyes in the visible range and their chemical and photostability are more limited. These are definitely important challenges to overcome, in order to increase the efficiency of dye-loaded NIR NPs for bioimaging applications.

4.5 Blinking

Organic fluorophores have the inherent property to blink due to their tendency to undergo numerous reactions that can alter their emission state. Intersystem crossing leading to the triplet state and electron transfer are two main mechanisms behind the off states observed for single dyes on the times scales between microseconds and milliseconds.[120] On the other hand, dye-based nanoparticles usually show continuous emission, because the blinking of individual dyes within the ensemble is averaged out. Thus, AIE-based polymer NPs were reported to show no blinking.[121] The same stable emission was reported for PLGA NPs

loaded with cyanine[57, 79] and PDI[22c] dyes. In this respect, dye-based polymer NPs are similar to conjugated polymer NPs, which also show continuous emission, especially those containing multiple chains per NP.[17a, 25] However, one report showed that smaller NPs, which are probably composed of a single conjugated polymer chain, do blink.[17a] In fact, it has been well established that immobilized single conjugated polymer molecules undergo light-induced blinking, which originates from ultra-fast exciton migration that quenches the whole polymer by single dark species.[122] The absence of blinking in NPs is considered as an advantage compared to QDs, which are well-known for their strong blinking behavior.[106] It enables robust particle tracking without interruptions produced by the off-states. However, new super-resolution microscopy techniques, such as direct stochastic optical reconstruction microscopy (dSTORM) require the capacity of nano-emitters to blink.[123] Recently, our group developed dye-loaded PLGA NPs that showed unprecedented on/off switching phenomena of up to 500 encapsulated rhodamine dyes (Fig. 11).[23] The reason for this collective switching of dyes was ultrafast exciton migration that couples all the encapsulated dyes together. In this case, a single dark species of rhodamine in a triplet or radical state was the energy trap for the whole ensemble of 500 dyes.[23] Using a dSTORM protocol, we were able to show that this blinking behavior could be used to separate two particles in space at distances below 100 nm and achieving super-localization up to 30 nm. We consider that the development of fluorescent NPs with controlled and robust blinking or switching behavior[23, 124] could open new possibilities in super-resolution imaging.

4.6 Surface chemistry and colloidal stability

Mastering surface chemistry for NPs is a key step towards their application in biological imaging.[125] On one hand the surface of NPs must present hydrophilic groups that can ensure their colloidal stability and minimize non-specific interactions with biological molecules. On the other, they should present the possibility to introduce specific interactions with molecules or cells of interest through antibodies, receptor ligands, etc. The surface chemistry of NPs clearly depends on the type of preparation method and the type of dyes they encapsulate. Thus, AIE dye assemblies after direct precipitation present a hydrophobic surface that cannot be directly functionalized. Therefore, polymers or lipid-polymer conjugates are used as encapsulating agents.[16] The most common approach is to use DSPE-PEG, which enables preparation of small NPs with a PEG shell preventing non-specific interactions. Functionalized DSPE-PEG with reactive groups, such as maleimide,[86] or biological ligands, such as folic acid,[69a] RGD,[86] TAT,[59a] NLS,[69b] etc at the PEG end can then be used to obtain specific functionalities. In our recent studies, we proposed a modular approach to particle surface chemistry based on common polymers such as PMMA, PLGA and PCL.[54b] First, polymers bearing single charged groups were precipitated with the dyes in order to obtain ultra-small polymer NPs (15 nm). Second, their surface was further covered by PEG bearing surfactants Tween 80 or Pluronic F127, which increased the NPs size only by a few nanometers but rendered them stable in salt media and prevented their interactions with serum proteins.[54b] It should be noted that such non-covalent approaches used for surface chemistry control in dye-loaded polymer NPs is not very different from those used for QDs and conjugated polymer NPs. Thus, both polymer-lipid conjugates and amphiphilic polymers were also successfully used for encapsulating QDs [8a, 126] and conjugated polymer NPs.[107–108] We have to stress that surface

modification that exploits amphiphilic polymers and lipid-PEG conjugates is not always very stable because of partial solubility of these components in water.[66a, 127] Therefore, it cannot be excluded that these polymers, bound to the particle surface by non-covalent interactions, fall off from NPs in biological environments. Therefore, strategies of surface modification employing covalent linkage are required, e.g. cross-linking as employed recently for conjugated polymers NPs[128] and in the case of polymeric micelles.[62a] In polymer NPs encapsulating organic dyes a further possibility is the covalent modification of the polymer forming the particle. For instance Law and co-workers, modified directly the chain end of PLGA to introduce PEG chains bearing SH-reactive maleimide groups.[57] Covalent modification can also be employed in emulsion co-polymerization with fluorescent monomers to control the NP surface.[39] Thus, Clavier et al. synthesized block-copolymers having a hydrophobic domain of polystyrene and BODIPY dyes followed by PAA and PEG blocks, which ensured preparation of PEG-coated polymer NPs.[96]

5 Bioimaging applications

Fluorescent nanoparticles are usually used either for detection of analytes (notably lab-on-a-chip), cellular or animal (*i.e. in vivo*) imaging. Though all these techniques prefer the brightest possible particles, they impose very different requirements. Thus, cellular imaging needs generally the smallest possible particles. Smaller particles can easier penetrate into the cells and provide less interference with the molecular processes studied. In contrast, *in vivo* studies prefer particles in a size range between 30 and 200 nm. Indeed, the particles should not be too large in order to prevent accumulation in liver or lungs and increased phagocytosis, but also not too small in order to avoid rapid clearance through the kidneys.[129] Second, cellular imaging requires dyes with emission colors in the range from blue to red (400-650 nm), where conventional microscopy systems show the optimized performance. In contrast, *in vivo* applications require NIR (>700 nm) or at least far red (600-700 nm) dyes, because of enhanced transparency of tissues in these spectral regions.[114] Dye-loaded NPs become an interesting alternative to dyes and quantum dots in bioimaging applications and offer new possibilities beyond bioimaging.

5.1 Cellular imaging

5.1.1 NP internalization into cells—Fluorescent NPs have been employed to visualize the mechanisms, pathways, and the parameters that govern NP entry into cells. This is especially important in view of the use of NPs for drug delivery applications. Generally, polymer NPs enter the cells by endocytosis, as it was for instance shown for our 40 nm PLGA NPs (Fig. 12A,B). Significant efforts were done to understand the effect of the particle size on the internalization. Schubert and coworkers found that PMMA NPs in the size range 100-200 nm show the fastest internalization and that while NPs < 200 nm were internalized through clathrin-dependent endocytosis, leading to their localization in endosomes and lysosomes, NPs > 300 nm were preferentially internalized through micropinocytosis.[130] Hoffmann et al used 25 nm and 100 nm PS NPs displaying different fluorescence lifetimes for comparing directly their uptake.[131] Ferrari et al. imaged cellular uptake of rhodamine B loaded PMMA NPs of 50, 100, and 200 nm using fluorescence intensity, flow cytometry, and microscopy.[33a] In this way the absolute number of NPs

could be determined and they were found to be localized in the perinuclear region indicating endocytotic pathways. The internalization kinetics were faster for smaller NPs. Especially the 50 nm NPs were also less strongly retained in the cells. In the same study the influence of the NP surface and notably its charge was also addressed. Positively charged particles showed the highest cellular uptake and also the highest retention especially for NPs ≥ 100 nm. This is in agreement with other studies[38] that showed, for example, higher cellular uptake of PMAO based NPs coated with the polycation chitosan.[70] To improve internalization, fusogenic peptides were grafted to the particle surface, as for instance was realized for TAT peptides.[69b, 132] Nevertheless, efficient delivery of polymer NPs inside the cells, and particularly into the cytosol, remains the bottleneck in the field of NPs in general and dye-loaded NPs in particular.

5.1.2 Receptor-specific targeting of cells—A second important field of application is the receptor-specific labeling of cells. In this aim, antibodies or small molecule ligands for an antigen expressed specifically or over-expressed by a given cell type are tethered to the surface of the NPs.[13] The most prominent example is the use of folate groups on the surface of NPs[49, 58a] to target folate receptors, which are typically over-expressed in cancer cells. For example, AIE based NPs showed increasing internalization in MCF-7 cancer cells with increasing folic acid content of the NP surface, while internalization in NIH3T3 cells was not increased.[69a] Higher specificity could notably be achieved using primary antibodies for targeting. In this way, using Herceptin and IgG2A11 antibodies conjugated to FRET NPs of different emission colors could be used to specifically target cells in mixtures of different cell types (Fig. 12B).[79] Other strategies for targeting include the modification with cyclic peptide RGD[133], lectins,[134] or aptamers.[135]

5.1.3 Long-term cell tracking—The particle nature of these probes allows their use for the tracking of cells over several generations. Indeed, as NPs are relatively stable objects that enter the cells by endocytosis, they remain there for a long time thus ensuring long-term staining of the cells. The majority of examples are focused on AIE-based NPs.[16, 59a, 69b, 136] Long-term tracking has been applied notably to dendritic cells[38] and different cancer cell lines,[59a, 132, 136] and allowed labeling over up to 7 generations. NPs of two different colors[79] or combination with unlabeled cells[136] made discrimination of different populations feasible.

5.1.4 Single-molecule and single-particle tracking—Single-molecule and single particle tracking help imaging biomolecules at work directly in living cells.[1c, 137] Though the state of the art single-molecule microscopy allows detection and tracking of single dyes and fluorescent proteins in cells, the signal to noise ratio and the tracking time are limited by their brightness and number of photons they deliver before photobleaching (~10^5). Moreover, the localization precision and speed directly depend on the brightness of the probe,[2] whereas, the excitation intensity should be limited on biological samples.[4b] Therefore, to increase the sensitivity in single molecule detection and tracking, the biomolecules are labeled with tandem copies of dyes or fluorescent proteins.[138] Dye-loaded NPs can be 10-1000 times brighter than dyes and fluorescent proteins and can emit >4×10^7 photons,[87] which make them particularly promising for these applications.

Though fluorescent polymeric beads have been used early-on in single molecule tracking,[139] this field is currently dominated by quantum dots.[8b] The probable reasons for this domination are their relatively small and reproducible size with very good monodispersity as well as well-developed surface chemistry. Relevant fluorescent organic nanoparticles based on conjugated polymers (Pdots) and dyes already showed that high brightness together with large number of delivered photons enable particle tracking with extreme precision for longer periods.[14e, 140] Moreover, extreme brightness of recently developed dye-loaded lipid NPs could even allow single particle tracking in vivo on zebrafish.[15b] In one recent report, 40 nm dye-loaded polymer NPs were compared to quantum dots in single particle tracking studies to evaluate the diffusion of membrane lipids.[141] It was shown that polymer NPs are a very interesting alternative to quantum dots in single particle tracking due to high brightness, photostability and non-blinking. Nevertheless, it is clear that this application is largely underexplored and the new generation of bright and small dye-loaded NPs should rapidly fill this gap.

5.2 In vivo imaging

Use of fluorescent dye-loaded NPs *in vivo* bears great potential, but implies also several challenges. In particular the biodistribution of the NPs and its development over time has to be considered. In contrast to small organic dyes, nanoparticles being administrated into the blood circulation can remain much longer times. This makes them promising for imaging blood vessels and circulation.[59b] [15b, 94b] This is notably important to understand the development of the cardiovascular system of embryos. Biodistribution studies of polymer NPs show that the clearance from blood circulation in healthy mice is usually accompanied by accumulation in organs such as liver, lungs and spleen, etc, as it was shown for PLGA-based NPs loaded with ICG.[77a] The circulation time of the nanoparticles can be prolonged through the modification with PEG.[77c, 79, 142] In these cases the stability of NPs *in vivo* becomes an important aspect. In one recent study, polymeric micelles of peptide-PEG block copolymer labeled with Cy5.5 and Cy7 derivatives were assembled into FRET NPs and further studied *in vivo*.[94d] The results showed that the FRET signal was observed within the experimental time (up to 96h), suggesting that these NPs remain intact and do not really dissociate after accumulation in organs (Fig. 13A,B). However, this type of study is still missing for all other types of polymer NPs, which would be very informative in the view of their *in vivo* applications. Importantly, the prolonged circulation of NPs offers the possibility of their accumulation in tumors either by EPR or by receptor-specific delivery. In fact, imaging tumors in small animals, mice in particular, is one of the most popular applications of fluorescent nanoparticles.[24] In this respect, the effect of particle size on accumulation into tumors is currently intensively studied.[101] In one example, NPs prepared by co-nanoprecipitation of the PLGA polymer with Cy7 (DiR) were studied on mice bearing two different xenograft tumor types, the HT29 (colorectal carcinoma) and the A2780 (ovarian carcinoma) cell lines. It was observed that small NP batches (d ~ 111 and 141 nm) accumulated efficiently in the human xenograft tumor tissue, while slightly larger NPs (d ~ 166 nm) were rapidly eliminated by the liver.[143] In order to further improve targeting to tumors, targeting groups especially folic acid,[77c, 144] but also various other groups as cholanic acid[94b] are implemented at the NP surface. Besides administration through the cardiovascular system, several reports have also shown that it is possible to administer NPs

through the lymphatic system.[70, 145] Dye-loaded NPs that are delivered into tumors can then in principle be used for following drug delivery[94a] or directly for treatment through photothermal therapy.[146]

Cell tracking based on fluorescent polymeric nanoparticles can also be extended to *in vivo* applications. This can be used for the imaging of tumor development, where, in one example, cancerous cells were first incubated with AIE-based NPs and then injected subcutaneously into mice and imaged over 21 days (Fig. 13C).[59a] A similar procedure based on NPs with polymerizable Rhodamine B has been used for monitoring the fate of stem cells, that were implanted in mouse brain lateral ventricles.[33b]

5.3 Biocompatibility, biodegradability and toxicity

A prerequisite for successful application is that the NPs modify the least possible the behavior of the biological system. This comprises, besides an appropriate size and surface chemistry already discussed above, the absence of toxicity. Cytotoxicity of fluorescent NPs is now nearly systematically evaluated for new dye loaded NP constructs. The results show that dye-loaded NPs typically show no significant toxicity at least up to NP concentrations in the nM range[23, 57, 59a, 79] and dye concentrations up to μM[23, 49, 86] or even tens of μM[58a, 58c]. This corresponds to concentrations far above those typically applied for labeling. Tests are most often performed for periods of 24 to 72 h, covering the time frame of many imaging applications. Furthermore, the encapsulation of the dyes inside the NPs tends to reduce the toxicity compared to the free dye.[86] It could also be shown that pegylated dye loaded PLGA NPs are hemocompatible, i.e. that they do not damage erythrocytes.[57] Taken together these results show that dye-loaded polymer NPs can be safely used for cellular imaging applications. However, up to date studies on the systemic toxicity of these NPs especially in dependence of the type of administration (intravenous, oral, subcutaneous, etc.) are largely missing. Indeed, *in vivo* studies often give the biodistribution of the NPs but are not carried out long enough to evaluate their toxicity on the whole body level. At the same time, one of the big advantages of dye-loaded polymer NPs over other types of fluorescent NPs as QDs, silica NPs, or conjugated polymer NPs, is that they can be made biodegradable through the choice of convenient biodegradable polymers like PLGA, PCL, etc as matrix materials. Dye-loaded NPs are thus currently the major candidates for applications of fluorescent NPs directly in a biomedical context, opening the way to actual theranostics.[147] Strategies have been developed for harvesting this potential while maintaining the performance of dye-loaded NPs.[148]

5.4 Emerging applications

Up to recently dye-loaded NPs have essentially been used as labels or as model systems that allow the visualization of the behavior of NPs in biological systems. However, currently several applications emerge that notably make use of dye-loaded NPs as fluorescent probes and combine fluorescence with other modalities.

First, a couple of approaches have been developed that allow modulating the fluorescence response of NPs depending on external stimuli and the presence of analytes. In these approaches typically a sensor dye and a reference dye are combined within NPs in order to

obtain a ratiometric response. The use of FRET between these dyes enables excitation of NPs at single wavelength and recording the two band ratiometric signal from donor and acceptor dyes. For example several types of sensors for reactive oxygen species (ROS) have been developed. Napp and coworkers doped PS NPs with palladium meso-tetraphenylporphyrin that is quenched in the presence of reactive oxygen species and an inert reference dye to measure the presence of ROS from the ratio of the two emissions and the fluorescence lifetimes.[149] Similar approaches have been applied to the sensing of temperature,[150] pH,[151] and analytes as Cu(II)[22a]. However, it should be noted that development of fluorescent probes based on dye-loaded polymer NPs is still at its infancy. Much more work is required to make them functioning well in biological media in order to be competitive with classical molecular fluorescent probes.

Second, the unique possibilities of combining different components within dye-loaded polymer NPs are also particularly interesting for integrating drugs and other active compounds. This especially concerns NPs built from biodegradable polymers, which can function as both drug-delivery carriers and contrast agents for in vivo imaging.[24] An exciting possibility is to directly monitor drug release *in situ* using these NPs, as it was realized using FRET between the encapsulated dyes and drugs, as it was recently shown using the anti-cancer drug doxorubicin as FRET acceptor.[67b] Dye-loaded NPs also have the potential to be used in photodynamic therapy and destroy cancer cells after receptor specific uptake upon radiation induced generation of ROS.[152] Here, we should also mention a recently proposed “see and treat” strategy using biodegradable polyacrylamide NPs loaded with NIR dye for bioimaging and a photosynthesizer for photodynamic therapy.[42] A further level of control can be achieved by controlling the delivery of active compounds using light absorbed by the dyes. In a recent example a photoactivatable polymer was combined with AIE motives in NPs loaded with DNA. After particle endocytosis ROS production upon irradiation led to particle degradation followed by cytosolic delivery of the DNA.[153] Combining different imaging and therapeutic modalities together with triggering mechanisms within polymer NPs open enormous possibilities for future theranostics. [147]

6 Conclusion and perspectives

Fluorescent dye-loaded polymer NPs, encapsulating a high number of fluorescent dyes, have made a huge leap forward over the last years fueled by the need for fluorescent probes that exceed the brightness of organic dyes, fluorescent proteins, and even quantum dots. This has led to the development of different approaches to overcome aggregation caused quenching, which limited the achievable brightness for dye-loaded NPs. The major strategies either exploit aggregation induced emission, where specially designed dyes become fluorescent in the aggregated state, or they aim at controlling the organization of dyes using modification with bulky groups, bulky hydrophobic counterions, or polymerization of dye monomers.

As summarized in Table 4, the key advantages of dye-loaded NPs are (1) much higher brightness compared to dyes and QDs; (2) broader absorption and emission range compared to QDs and conjugated polymer NPs, and (3) biodegradability, in contrast to QDs and conjugated polymer NPs. Moreover, there is still a room to improve the brightness of dye-

Europe PMC Funders Author Manuscripts

loaded polymer NPs notably by increasing the dye loading and developing efficient strategies against ACQ. These advantages stimulated a number of bioimaging applications *in vitro* on cells and *in vivo* on small animals. However, several problems of current dye-loaded polymer NPs should be addressed before they can be broadly used in bioimaging applications as dyes, fluorescent proteins and quantum dots. First, their hydrodynamic diameter is larger than that of QDs and conjugated polymer NPs, so that for efficient use in many cellular applications it should be decreased to the 5-15 nm range. This is particular important for detection and tracking of single molecules and for rapidly expanding super-resolution imaging, where the particle size should be comparable to that of biomolecules. Second, they are not as monodisperse as QDs, so that their brightness and diffusion coefficient are more heterogeneous, limiting quantitative imaging applications. Therefore, the protocols for their preparation have to be improved accordingly and they should become highly reproducible independently of the user. In this case, the results in biological samples obtained in different laboratories could be directly compared, as it is currently done with dyes and commercial QDs. Third, photostability of dye-loaded NPs has to be more systematically evaluated, which should help to design NPs delivering the largest possible number of photons before photobleaching. Fourth, their blinking should be better addressed and controlled, so that NPs with constant emission could be applied for particle tracking, while those with complete on/off switching could be used in super-resolution imaging. Finally, surface chemistry and colloidal stability remain a challenge. A general problem of dye-loaded polymer NPs is non-specific interactions in biological media. Designing a thin non-interacting hydrophilic shell at the surface of small polymer NPs will be important both for stability in biological media and for achieving high specificity to biomolecular targets *in vitro* and *in vivo*. Moreover, a particular attention should be paid to preventing any leaching of the encapsulated dyes from the particle to biological media, which would minimize artifacts and maximize the signal to background ratio. Therefore, the synthetic protocols must ensure the best encapsulation of the dyes inside NPs, followed by efficient purification and reliable stability evaluation. Bioconjugation techniques must be further improved, so that it would become possible to covalently graft the desired number of specific ligands to the particle surface and ensure their exposure to the target. Here, both pre- and post-functionalization protocols using robust and orthogonal bioconjugation reactions should be explored in full.

Once all these points are systematically addressed, we expect dye-loaded polymer NPs to become a common tool on the bench of researchers in the biological and biomedical fields. They would not only replace the existing molecular and nanoparticle tools, but stimulate new applications, where fluorescence brightness and biodegradability matter the most. As these NPs use polymer matrices of typical drug-delivery nanocarriers, the progress in dye-loaded NPs and understanding of their interaction with biological systems are readily extendable to therapeutic modalities and to any other contrast agents, facilitating routes to theranostics based on biodegradable materials.

Acknowledgment

This work was supported by ERC Consolidator grant BrightSens 648528. Jurga Valanciunaite is acknowledged for proofreading the manuscript.

Europe PMC Funders Author Manuscripts

References

[1]. a) Giepmans BNG, Adams SR, Ellisman MH, Tsien RY. Science. 2006; 312:217–224. [PubMed: 16614209] b) Nelson AJ, Hess ST. J Microsc-Oxford. 2014; 254:1–8.c) Kusumi A, Tsunoyama TA, Hirosawa KM, Kasai RS, Fujiwara TK. Nat Chem Biol. 2014; 10:524–532. [PubMed: 24937070]

[2]. Deschout H, Zanacchi FC, Mlodzianoski M, Diaspro A, Bewersdorf J, Hess ST, Braeckmans K. Nat Methods. 2014; 11:253–266. [PubMed: 24577276]

[3]. a) Ha T, Tinnefeld P. Annual Review of Physical Chemistry. 2012; 63:595–617.b) Stennett EMS, Ciuba MA, Levitus M. Chemical Society Reviews. 2014; 43:1057–1075. [PubMed: 24141280]

[4]. a) Dixit R, Cyr R. The Plant Journal. 2003; 36:280–290. [PubMed: 14535891] b) Magidson V, Khodjakov A. Methods Cell Biol. 2013:114.c) Schilling Z, Frank E, Magidson V, Wason J, Lončarek J, Boyer K, Wen J, Khodjakov A. J Microsc-Oxford. 2012; 246:160–167.

[5]. a) Wolfbeis OS. Chemical Society Reviews. 2015; 44:4743–4768. [PubMed: 25620543] b) Howes PD, Chandrawati R, Stevens MM. Science. 2014; 346:1247390. [PubMed: 25278614]

[6]. a) Owens DE, Peppas NA. International Journal of Pharmaceutics. 2006; 307:93–102. [PubMed: 16303268] b) Nel AE, Mädler L, Velegol D, Xia T, Hoek EMV, Somasundaran P, Klaessig F, Castranova V, Thompson M. Nat Mater. 2009; 8:543–557. [PubMed: 19525947] c) Monopoli MP, Åberg C, Salvati A, Dawson KA. Nat Nano. 2012; 7:779–786.

[7]. a) Wang M, Thanou M. Pharmacological Research. 2010; 62:90–99. [PubMed: 20380880] b) Morachis JM, Mahmoud EA, Almutairi A. Pharmacological Reviews. 2012; 64:505–519. [PubMed: 22544864]

[8]. a) Michalet X, Pinaud FF, Bentolila LA, Tsay JM, Doose S, Li JJ, Sundaresan G, Wu AM, Gambhir SS, Weiss S. Science. 2005; 307:538–544. [PubMed: 15681376] b) Pinaud F, Clarke S, Sittner A, Dahan M. Nat Methods. 2010; 7:275–285. [PubMed: 20354518]

[9]. Genovese D, Rampazzo E, Bonacchi S, Montalti M, Zaccheroni N, Prodi L. Nanoscale. 2014; 6:3022–3036. [PubMed: 24531884]

[10]. Gnach A, Bednarkiewicz A. Nano Today. 2012; 7:532–563.

[11]. a) Antelman J, Ebenstein Y, Dertinger T, Michalet X, Weiss S. J Phys Chem C. 2009; 113:11541–11545.b) Chen O, Zhao J, Chauhan VP, Cui J, Wong C, Harris DK, Wei H, Han H-S, Fukumura D, Jain RK, Bawendi MG. Nat Mater. 2013; 12:445–451. [PubMed: 23377294] c) Chen Y, Vela J, Htoon H, Casson JL, Werder DJ, Bussian DA, Klimov VI, Hollingsworth JA. J Am Chem Soc. 2008; 130:5026–5027. [PubMed: 18355011]

[12]. Sperling RA, Parak WJ. Phil Trans R Soc A. 2010; 368:1333–1383. [PubMed: 20156828]

[13]. Peng H-S, Chiu DT. Chemical Society Reviews. 2015; 44:4699–4722. [PubMed: 25531691]

[14]. a) Kaeser A, Schenning APHJ. Adv Mater. 2010; 22:2985–2997. [PubMed: 20535737] b) Schill J, Schenning APHJ, Brunsveld L. Macromol Rapid Commun. 2015; 36:1306–1321. [PubMed: 25990315] c) Yao, H. Advanced Fluorescence Reporters in Chemistry and Biology II. Demchenko, AP., editor. Springer Berlin Heidelberg; 2010. p. 285-304.d) Hamdan S, Dumke JC, El-Zahab B, Das S, Boldor D, Baker GA, Warner IM. J Colloid Interface Sci. 2015; 446:163–169. [PubMed: 25666457] e) Genin E, Gao Z, Varela JA, Daniel J, Bsaibess T, Gosse I, Groc L, Cognet L, Blanchard-Desce M. Adv Mater. 2014; 26:2258–2261. [PubMed: 24497445] f) Gaiduk A, Yorulmaz M, Ishow E, Orrit M. ChemPhysChem. 2012; 13:946–951. [PubMed: 22184072] g) Fery-Forgues S. Nanoscale. 2013; 5:8428–8442. [PubMed: 23900346]

[15]. a) Texier I, Goutayer M, Da Silva A, Guyon L, Djaker N, Josserand V, Neumann E, Bibette J, Vinet F. Journal of biomedical optics. 2009; 14:054005. [PubMed: 19895107] b) Kilin VN, Anton H, Anton N, Steed E, Vermot J, Vandamme TE, Mely Y, Klymchenko AS. Biomaterials. 2014; 35:4950–4957. [PubMed: 24661553]

[16]. Li K, Liu B. Chemical Society Reviews. 2014; 43:6570–6597. [PubMed: 24792930]

[17]. a) Wu C, Bull B, Szymanski C, Christensen K, McNeill J. ACS nano. 2008; 2:2415–2423. [PubMed: 19206410] b) Pecher J, Mecking S. Chemical Reviews. 2010; 110:6260–6279. [PubMed: 20684570]

Europe PMC Funders Author Manuscripts

[18]. a) Makadia HK, Siegel SJ. Polymers. 2011; 3:1377–1397. [PubMed: 22577513] b) Danhier F, Ansorena E, Silva JM, Coco R, Le Breton A, Preat V. Journal of Controlled Release. 2012; 161:505–522. [PubMed: 22353619]

[19]. a) Rao JP, Geckeler KE. Progress in Polymer Science. 2011; 36:887–913.b) Schubert S, Delaney JT, Schubert US. Soft Matter. 2011; 7:1581–1588.c) Duncan R, Richardson SCW. Mol Pharmaceutics. 2012; 9:2380–2402.d) Delplace V, Couvreur P, Nicolas J. Polym Chem. 2014; 5:1529–1544.

[20]. Lavis LD, Raines RT. ACS Chemical Biology. 2008; 3:142–155. [PubMed: 18355003]

[21]. a) Wartenberg N, Raccurt O, Imbert D, Mazzanti M, Bourgeat-Lami E. Journal of Materials Chemistry C. 2013; 1:2061–2068.b) Hughes JM, Budd PM, Grieve A, Dutta P, Tiede K, Lewis J. Journal of Applied Polymer Science. 2015:132.c) Rasanen M, Takalo H, Soukka T, Haapakka K, Kankare J. Journal of Luminescence. 2015; 160:128–133.d) Desbiens J, Bergeron B, Patry M, Ritcey AM. J Colloid Interface Sci. 2012; 376:12–19. [PubMed: 22459030]

[22]. a) Méallet-Renault R, Hérault A, Vachon J-J, Pansu RB, Amigoni-Gerbier S, Larpent C. Photochem Photobiol Sci. 2006; 5:300–310. [PubMed: 16520865] b) Tian Z, Shaller AD, Li ADQ. Chem Commun. 2009:180–182.c) Trofymchuk K, Reisch A, Shulov I, Mely Y, Klymchenko AS. Nanoscale. 2014; 6:12934–12942. [PubMed: 25233438]

[23]. Reisch A, Didier P, Richert L, Oncul S, Arntz Y, Mely Y, Klymchenko AS. Nature Communications. 2014; 5:4089.

[24]. Vollrath A, Schubert S, Schubert US. Journal of Materials Chemistry B. 2013; 1:1994–2007.

[25]. Wu C, Chiu DT. Angewandte Chemie - International Edition. 2013; 52:3086–3109. [PubMed: 23307291]

[26]. Alivisatos AP. Science. 1996; 271:933–937.

[27]. a) Vauthier C, Bouchemal K. Pharmaceutical Research. 2009; 26:1025–1058. [PubMed: 19107579] b) Landfester K, Musyanovych A, Mailaender V. Journal of Polymer Science Part a-Polymer Chemistry. 2010; 48:493–515.

[28]. Zhang X, Wang K, Liu M, Zhang X, Tao L, Chen Y, Wei Y. Nanoscale. 2015; 7:11486–11508. [PubMed: 26010238]

[29]. Odian, G. Principles of Polymerization. 4th ed. Wiley-Interscience; 2004.

[30]. a) Harkins WD. J Am Chem Soc. 1947; 69:1428–1444. [PubMed: 20249728] b) Smith WV, Ewart RH. The Journal of Chemical Physics. 1948; 16:592–599.c) Thickett SC, Gilbert RG. Polymer. 2007; 48:6965–6991.

[31]. Ni H, Du Y, Ma G, Nagai M, Omi S. Macromolecules. 2001; 34:6577–6585.

[32]. a) Zhang X, Zhang X, Yang B, Liu M, Liu W, Chen Y, Wei Y. Polym Chem. 2013; 5:399–404.b) Liu M, Zhang X, Yang B, Deng F, Li Z, Wei J, Zhang X, Wei Y. Applied Surface Science. 2014; 322:155–161.

[33]. a) Ferrari R, Lupi M, Falcetta F, Bigini P, Paolella K, Fiordaliso F, Bisighini C, Salmona M, D'Incalci M, Morbidelli M, Moscatelli D, et al. Nanotechnology. 2014:25.b) Cova L, Bigini P, Diana V, Sitia L, Ferrari R, Pesce RM, Khalaf R, Bossolasco P, Ubezio P, Lupi M, Tortarolo M, et al. Nanotechnology. 2013; 24:245603. [PubMed: 23690139]

[34]. a) Wang X, Xu S, Xu W. Phys Chem Chem Phys. 2011; 13:1560–1567. [PubMed: 21103543] b) Thielbeer F, Chankeshwara SV, Bradley M. Biomacromolecules. 2011; 12:4386–4391. [PubMed: 22059964]

[35]. Martin V, Banuelos J, Enciso E, Arbeloa IL, Costela A, Garcia-Moreno I. Journal of Physical Chemistry C. 2011; 115:3926–3933.

[36]. Shaller AD, Wan W, Zhao B, Li ADQ. Chem Eur J. 2014; 20:12165–12171. [PubMed: 25111357]

[37]. López Arbeloa F, Bañuelos Prieto J, López Arbeloa I, Costela A, García-Moreno I, Gómez C, Amat-Guerri F, Liras M, Sastre R. Photochemistry and Photobiology. 2003; 78:30–36. [PubMed: 12929745]

[38]. Zupke O, Distler E, Baumann D, Strand D, Meyer RG, Landfester K, Herr W, Mailänder V. Biomaterials. 2010; 31:7086–7095. [PubMed: 20573395]

[39]. Sauer R, Turshatov A, Baluschev S, Landfester K. Macromolecules. 2012; 45:3787–3796.

[40]. Grazon C, Rieger J, Méallet-Renault R, Clavier G, Charleux B. Macromol Rapid Commun. 2011; 32:699–705. [PubMed: 21491536]

[41]. Monguzzi A, Frigoli M, Larpent C, Meinardi F. RSC Adv. 2012; 2:11731–11736.

[42]. Wang S, Kim G, Lee Y-EK, Hah HJ, Ethirajan M, Pandey RK, Kopelman R. ACS nano. 2012; 6:6843–6851. [PubMed: 22702416]

[43]. a) Landfester K. Adv Mater. 2001; 13:765–768.b) Antonietti M, Landfester K. Progress in Polymer Science. 2002; 27:689–757.

[44]. a) Zhuang D, Hogen-Esch TE. Macromolecules. 2010; 43:8170–8176.b) Chen J, Zhang P, Fang G, Yi P, Yu X, Li X, Zeng F, Wu S. Journal of Physical Chemistry B. 2011; 115:3354–3362.

[45]. a) Antonietti M, Basten R, Lohmann S. Macromol Chem Phys. 1995; 196:441–466.b) Candau F, Pabon M, Anquetil J-Y. Colloids and Surfaces A: Physicochemical and Engineering Aspects. 1999; 153:47–59.

[46]. Gao HF, Zhao YQ, Fu SK, Li B, Li MQ. Colloid and Polymer Science. 2002; 280:653–660.

[47]. Ouadahi K, Allard E, Oberleitner B, Larpent C. Journal of Polymer Science Part a-Polymer Chemistry. 2012; 50:314–328.

[48]. Galindo-Rodriguez S, Allemann E, Fessi H, Doelker E. Pharmaceutical Research. 2004; 21:1428–1439. [PubMed: 15359578]

[49]. Geng J, Li K, Qin W, Ma L, Gurzadyan GG, Tang BZ, Liu B. Small. 2013; 9:2012–2019. [PubMed: 23404950]

[50]. a) Jin C, Bai L, Wu H, Song W, Guo G, Dou K. Pharmaceutical Research. 2009; 26:1776–1784. [PubMed: 19384463] b) Eliza G, Alf L, Nathalie U, Philippe M, Janina L, Joël C, Pierre L. Nanotechnology. 2006; 17:2546. [PubMed: 21727503]

[51]. a) Fessi H, Puisieux F, Devissaguet JP, Ammoury N, Benita S. International Journal of Pharmaceutics. 1989; 55:R1–R4.b) Mora-Huertas CE, Fessi H, Elaissari A. Advances in Colloid and Interface Science. 2011; 163:90–122. [PubMed: 21376297]

[52]. a) D'Addio SM, Prud'homme RK. Advanced Drug Delivery Reviews. 2011; 63:417–426. [PubMed: 21565233] b) Ganachaud F, Katz JL. ChemPhysChem. 2005; 6:209–216. [PubMed: 15751338]

[53]. Lince F, Marchisio DL, Barresi AA. J Colloid Interface Sci. 2008; 322:505–515. [PubMed: 18402975]

[54]. a) Nehilla BJ, Allen PG, Desai TA. ACS nano. 2008; 2:538–544. [PubMed: 19206580] b) Reisch A, Runser A, Arntz Y, Mély Y, Klymchenko AS. ACS Nano. 2015; 9:5104–5116. [PubMed: 25894117]

[55]. a) Lepeltier E, Bourgaux C, Couvreur P. Advanced Drug Delivery Reviews. 2014; 71:86–97. [PubMed: 24384372] b) Danhier F, Lecouturier N, Vroman B, Jérôme C, Marchand-Brynaert J, Feron O, Préat V. Journal of Controlled Release. 2009; 133:11–17. [PubMed: 18950666] c) Barichello JM, Morishita M, Takayama K, Nagai T. Drug Development and Industrial Pharmacy. 1999; 25:471–476. [PubMed: 10194602]

[56]. Beck-Broichsitter M, Rytting E, Lebhardt T, Wang X, Kissel T. European Journal of Pharmaceutical Sciences. 2010; 41:244–253. [PubMed: 20600881]

[57]. Wagh A, Qian SY, Law B. Bioconjugate Chem. 2012; 23:981–992.

[58]. a) Diao X, Li W, Yu J, Wang X, Zhang X, Yang Y, An F, Liu Z, Zhang X. Nanoscale. 2012; 4:5373–5377. [PubMed: 22814892] b) Yang Y, An F, Liu Z, Zhang X, Zhou M, Li W, Hao X, Lee C-S, Zhang X. Biomaterials. 2012; 33:7803–7809. [PubMed: 22819497] c) Yu J, Diao X, Zhang X, Chen X, Hao X, Li W, Zhang X, Lee C-S. Small. 2014; 10:1125–1132. [PubMed: 24318966]

[59]. a) Li K, Qin W, Ding D, Tomczak N, Geng J, Liu R, Liu J, Zhang X, Liu H, Liu B, Tang BZ. Sci Rep. 2013:3.b) Tao Z, Hong G, Shinji C, Chen C, Diao S, Antaris AL, Zhang B, Zou Y, Dai H. Angew Chem Int Ed. 2013; 52:13002–13006.

[60]. Ma C, Ling Q, Xu S, Zhu H, Zhang G, Zhou X, Chi Z, Liu S, Zhang Y, Xu J. Macromol Biosci. 2014; 14:235–243. [PubMed: 24105985]

[61]. a) Nishiyama N, Kataoka K. Pharmacol Ther. 2006; 112:630–648. [PubMed: 16815554] b) Kwon GS, Kataoka K. Advanced Drug Delivery Reviews. 2012; 64(Supplement):237–245.c) Riess G. Progress in Polymer Science. 2003; 28:1107–1170.

[62]. a) Sun G, Berezin MY, Fan J, Lee H, Ma J, Zhang K, Wooley KL, Achilefu S. Nanoscale. 2010; 2:548–558. [PubMed: 20644758] b) Wu W-C, Chen C-Y, Tian Y, Jang S-H, Hong Y, Liu Y, Hu R, Tang BZ, Lee Y-T, Chen C-T, Chen W-C, et al. Adv Funct Mater. 2010; 20:1413–1423.c) Robin MP, O'Reilly RK. Polym Int. 2015; 64:174–182.

[63]. Mortensen K, Brown W. Macromolecules. 1993; 26:4128–4135.

[64]. a) Lu H, Su F, Mei Q, Tian Y, Tian W, Johnson RH, Meldrum DR. J Mater Chem. 2012; 22:9890–9900. [PubMed: 23397360] b) Miki K, Oride K, Inoue S, Kuramochi Y, Nayak RR, Matsuoka H, Harada H, Hiraoka M, Ohe K. Biomaterials. 2010; 31:934–942. [PubMed: 19853909]

[65]. a) Hamilton SK, Harth E. ACS nano. 2009; 3:402–410. [PubMed: 19236078] b) Bian T, Wang C, Lu Z, Xie R, Yang Q-Z, Wu L-Z, Tung C-H, Liu Z, Yin Y, Zhang T. Small. 2015; 11:1644–1648. [PubMed: 25504669]

[66]. a) Bae YH, Yin HQ. Journal of Controlled Release. 2008; 131:2–4. [PubMed: 18625275] b) Chen HT, Kim SW, Li L, Wang SY, Park K, Cheng JX. P Natl Acad Sci USA. 2008; 105:6596–6601.

[67]. a) Yang Z, Yuan Y, Jiang R, Fu N, Lu X, Tian C, Hu W, Fan Q, Huang W. Polym Chem. 2014; 5:1372–1380.b) Chen J-I, Wu W-C. Macromol Biosci. 2013; 13:623–632. [PubMed: 23512927] c) Zhang Y, Chen Y, Li X, Zhang J, Chen J, Xu B, Fu X, Tian W. Polym Chem. 2014; 5:3824–3830.

[68]. a) Gustafson TP, Lim YH, Flores JA, Heo GS, Zhang F, Zhang S, Samarajeewa S, Raymond JE, Wooley KL. Langmuir. 2014; 30:631–641. [PubMed: 24392760] b) Robin MP, Raymond JE, O'Reilly RK. Mater Horiz. 2014; 2:54–59.

[69]. a) Li K, Jiang Y, Ding D, Zhang X, Liu Y, Hua J, Feng S-S, Liu B. Chem Commun. 2011; 47:7323–7325.b) Qin W, Li K, Feng G, Li M, Yang Z, Liu B, Tang BZ. Adv Funct Mater. 2014; 24:635–643.

[70]. Lee Y-D, Lim C-K, Kim S, Kwon IC, Kim J. Adv Funct Mater. 2010; 20:2786–2793.

[71]. Macdonald RI. J Biol Chem. 1990; 265:13533–13539. [PubMed: 2380172]

[72]. Klymchenko AS, Roger E, Anton N, Anton H, Shulov I, Vermot J, Mely Y, Vandamme TF. RSC Adv. 2012; 2:11876–11886.

[73]. Errede LA, Hanson SC. Journal of Applied Polymer Science. 1994; 54:619–647.

[74]. Zhu HG, McShane MJ. J Am Chem Soc. 2005; 127:13448–13449. [PubMed: 16190679]

[75]. Behnke T, Wurth C, Laux EM, Hoffmann K, Resch-Genger U. Dyes Pigment. 2012; 94:247–257.

[76]. Greenspan P, Mayer EP, Fowler SD. J Cell Biol. 1985; 100:965–973. [PubMed: 3972906]

[77]. a) Saxena V, Sadoqi M, Shao J. International Journal of Pharmaceutics. 2006; 308:200–204. [PubMed: 16386861] b) Zheng CF, Zheng MB, Gong P, Jia DX, Zhang PF, Shi BH, Sheng ZH, Ma YF, Cai LT. Biomaterials. 2012; 33:5603–5609. [PubMed: 22575835] c) Ma Y, Sadoqi M, Shao J. International Journal of Pharmaceutics. 2012; 436:25–31. [PubMed: 22692077]

[78]. Rodriguez VB, Henry SM, Hoffman AS, Stayton PS, Li XD, Pun SH. Journal of biomedical optics. 2008:13.

[79]. Wagh A, Jyoti F, Mallik S, Qian S, Leclerc E, Law B. Small. 2013; 9:2129–2139. [PubMed: 23359548]

[80]. Kasha M, Rawls HR, El-Bayoumi MA. Pure Appl Chem. 1965; 11:371–392.

[81]. Wurthner F, Kaiser TE, Saha-Moller CR. Angewandte Chemie-International Edition. 2011; 50:3376–3410. [PubMed: 21442690]

[82]. Luo JD, Xie ZL, Lam JWY, Cheng L, Chen HY, Qiu CF, Kwok HS, Zhan XW, Liu YQ, Zhu DB, Tang BZ. Chem Commun. 2001:1740–1741.

[83]. An BK, Kwon SK, Jung SD, Park SY. J Am Chem Soc. 2002; 124:14410. [PubMed: 12452716]

[84]. Grabowski ZR, Rotkiewicz K, Rettig W. Chemical Reviews. 2003; 103:3899–4031. [PubMed: 14531716]

[85]. Hong YN, Lam JWY, Tang BZ. Chemical Society Reviews. 2011; 40:5361–5388. [PubMed: 21799992]

[86]. Wang D, Qian J, He S, Park JS, Lee K-S, Han S, Mu Y. Biomaterials. 2011; 32:5880–5888. [PubMed: 21601279]

[87]. Li K, Zhu ZS, Cai PQ, Liu RR, Tomczak N, Ding D, Liu J, Qin W, Zhao ZJ, Hu Y, Chen XD, et al. Chem Mater. 2013; 25:4181–4187.

[88]. a) Margineanu A, Hofkens J, Cotlet M, Habuchi S, Stefan A, Qu JQ, Kohl C, Mullen K, Vercammen J, Engelborghs Y, Gensch T, et al. Journal of Physical Chemistry B. 2004; 108:12242–12251.b) Weil T, Vosch T, Hofkens J, Peneva K, Mullen K. Angewandte Chemie-International Edition. 2010; 49:9068–9093. [PubMed: 20973116] c) Wurthner F. Chem Commun. 2004:1564–1579.

[89]. a) Langhals H. Helvetica Chimica Acta. 2005; 88:1309–1343.b) Langhals H, Ismael R, Yuruk O. Tetrahedron. 2000; 56:5435–5441.

[90]. Colby KA, Burdett JJ, Frisbee RF, Zhu L, Dillon RJ, Bardeen CJ. J Phys Chem A. 2010; 114:3471–3482. [PubMed: 20170138]

[91]. a) Yao H, Ashiba K. RSC Adv. 2011; 1:834–838.b) Yao H, Yamashita M, Kimura K. Langmuir. 2009; 25:1131–1137. [PubMed: 19086783]

[92]. a) Bwambok DK, El-Zahab B, Challa SK, Li M, Chandler L, Baker GA, Warner IM. ACS nano. 2009; 3:3854–3860. [PubMed: 19928781] b) Jordan AN, Das S, Siraj N, de Rooy SL, Li M, El-Zahab B, Chandler L, Baker GA, Warner IM. Nanoscale. 2012; 4:5031–5038. [PubMed: 22766774]

[93]. Breul AM, Hager MD, Schubert US. Chemical Society Reviews. 2013; 42:5366–5407. [PubMed: 23482971]

[94]. a) Kim K, Kim JH, Park H, Kim YS, Park K, Nam H, Lee S, Park JH, Park RW, Kim IS, Choi K, et al. Journal of Controlled Release. 2010; 146:219–227. [PubMed: 20403397] b) Na JH, Koo H, Lee S, Min KH, Park K, Yoo H, Lee SH, Park JH, Kwon IC, Jeong SY, Kim K. Biomaterials. 2011; 32:5252–5261. [PubMed: 21513975] c) Mackiewicz N, Nicolas J, Handké N, Noiray M, Mougin J, Daveu C, Lakkireddy HR, Bazile D, Couvreur P. Chem Mat. 2014; 26:1834–1847.d) Morton SW, Zhao X, Quadir MA, Hammond PT. Biomaterials. 2014; 35:3489–3496. [PubMed: 24477190]

[95]. Zhang X, Chen ZJ, Wurthner F. J Am Chem Soc. 2007; 129:4886–+. [PubMed: 17402739]

[96]. Grazon C, Rieger J, Méallet-Renault R, Charleux B, Clavier G. Macromolecules. 2013; 46:5167–5176.

[97]. Grazon C, Rieger J, Charleux B, Clavier G, Meallet-Renault R. Journal of Physical Chemistry C. 2014; 118:13945–13952.

[98]. Zhang X, Liu M, Yang B, Zhang X, Chi Z, Liu S, Xu J, Wei Y. Polym Chem. 2013; 4:5060–5064.

[99]. Zhao YM, Wu Y, Yan GW, Zhang K. RSC Adv. 2014; 4:51194–51200.

[100]. a) Chan WCW, Nie SM. Science. 1998; 281:2016–2018. [PubMed: 9748158] b) Burda C, Chen XB, Narayanan R, El-Sayed MA. Chemical Reviews. 2005; 105:1025–1102. [PubMed: 15826010]

[101]. Cabral H, Matsumoto Y, Mizuno K, Chen Q, Murakami M, Kimura M, Terada Y, Kano MR, Miyazono K, Uesaka M, Nishiyama N, et al. Nat Nano. 2011; 6:815–823.

[102]. Govender T, Stolnik S, Garnett MC, Illum L, Davis SS. Journal of Controlled Release. 1999; 57:171–185. [PubMed: 9971898]

[103]. Würth C, Grabolle M, Pauli J, Spieles M, Resch-Genger U. Analytical Chemistry. 2011; 83:3431–3439. [PubMed: 21473570]

[104]. a) Nie SM, Chiu DT, Zare RN. Science. 1994; 266:1018–1021. [PubMed: 7973650] b) Yang XD, Lee CL, Westenhoff S, Zhang XP, Greenham NC. Adv Mater. 2009; 21:916–+.

[105]. Zondervan R, Kulzer F, Orlinskii SB, Orrit M. Journal of Physical Chemistry A. 2003; 107:6770–6776.

[106]. Frantsuzov P, Kuno M, Janko B, Marcus RA. Nature Physics. 2008; 4:519–522.

[107]. Wu C, Schneider T, Zeigler M, Yu J, Schiro PG, Burnham DR, McNeill JD, Chiu DT. J Am Chem Soc. 2010; 132:15410–15417. [PubMed: 20929226]

[108]. Howes P, Green M, Levitt J, Suhling K, Hughes M. J Am Chem Soc. 2010; 132:3989–3996. [PubMed: 20175539]

[109]. Hashim Z, Howes P, Green M. J Mater Chem. 2011; 21:1797–1803.

Europe PMC Funders Author Manuscripts

[110]. Saxena V, Sadoqi M, Shao J. Journal of Photochemistry and Photobiology B-Biology. 2004; 74:29–38.

[111]. Montalti M, Battistelli G, Cantelli A, Genovese D. Chem Commun. 2014; 50:5326–5329.

[112]. van Sark W, Frederix P, Van den Heuvel DJ, Gerritsen HC, Bol AA, van Lingen JNJ, Donega CD, Meijerink A. Journal of Physical Chemistry B. 2001; 105:8281–8284.

[113]. Martin C, Bhattacharyya S, Patra A, Douhal A. Photochem Photobiol Sci. 2014; 13:1241–1252. [PubMed: 24969364]

[114]. a) Frangioni JV. Current Opinion in Chemical Biology. 2003; 7:626–634. [PubMed: 14580568] b) Weissleder R. Nature Biotechnology. 2001; 19:316–317.

[115]. Zhao QL, Li K, Chen SJ, Qin AJ, Ding D, Zhang S, Liu Y, Liu B, Sun JZ, Tang B. J Mater Chem. 2012; 22:15128–15135.

[116]. Geng J, Zhu Z, Qin W, Ma L, Hu Y, Gurzadyan GG, Tang BZ, Liu B. Nanoscale. 2014; 6:939–945. [PubMed: 24284804]

[117]. Rong Y, Wu C, Yu J, Zhang X, Ye F, Zeigler M, Gallina ME, Wu I-C, Zhang Y, Chan Y-H, Sun W, et al. ACS nano. 2013; 7:376–384. [PubMed: 23282278]

[118]. Chan WCW, Maxwell DJ, Gao XH, Bailey RE, Han MY, Nie SM. Curr Opin Biotechnol. 2002; 13:40–46. [PubMed: 11849956]

[119]. Jin Y, Ye F, Zeigler M, Wu C, Chiu DT. ACS nano. 2011; 5:1468–1475. [PubMed: 21280613]

[120]. a) Dickson RM, Cubitt AB, Tsien RY, Moerner WE. Nature. 1997; 388:355–358. [PubMed: 9237752] b) Vogelsang J, Kasper R, Steinhauer C, Person B, Heilemann M, Sauer M, Tinnefeld P. Angewandte Chemie-International Edition. 2008; 47:5465–5469. [PubMed: 18601270] c) Yeow EKL, Melnikov SM, Bell TDM, De Schryver FC, Hofkens J. Journal of Physical Chemistry A. 2006; 110:1726–1734.

[121]. Ding D, Li K, Liu B, Tang BZ. Accounts Chem Res. 2013; 46:2441–2453.

[122]. a) Bout DAV, Yip W-T, Hu D, Fu D-K, Swager TM, Barbara PF. Science. 1997; 277:1074–1077.b) Thomas SW, Joly GD, Swager TM. Chemical Reviews. 2007; 107:1339–1386. [PubMed: 17385926]

[123]. a) van de Linde S, Heilemann M, Sauer M. Annual Review of Physical Chemistry. 2012; 63:519–540.b) Rust MJ, Bates M, Zhuang XW. Nat Methods. 2006; 3:793–795. [PubMed: 16896339]

[124]. a) Zhu M-Q, Zhang G-F, Li C, Li Y-J, Aldred MP, Li ADQ. J Innov Opt Health Sci. 2011; 04:395–408.b) Rampazzo E, Bonacchi S, Genovese D, Juris R, Montalti M, Paterlini V, Zaccheroni N, Dumas-Verdes C, Clavier G, Méallet-Renault R, Prodi L. J Phys Chem C. 2014; 118:9261–9267.c) Trofymchuk K, Prodi L, Reisch A, Mély Y, Altenhöner K, Mattay J, Klymchenko AS. The Journal of Physical Chemistry Letters. 2015; 6:2259–2264. [PubMed: 26266601]

[125]. Tonga GY, Saha K, Rotello VM. Adv Mater. 2014; 26:359–370. [PubMed: 24105763]

[126]. Medintz IL, Uyeda HT, Goldman ER, Mattoussi H. Nat Mater. 2005; 4:435–446. [PubMed: 15928695]

[127]. Kastantin M, Ananthanarayanan B, Karmali P, Ruoslahti E, Tirrell M. Langmuir. 2009; 25:7279–7286. [PubMed: 19358585]

[128]. Yu J, Wu C, Zhang X, Ye F, Gallina ME, Rong Y, Wu I-C, Sun W, Chan Y-H, Chiu DT. Adv Mater. 2012; 24:3498–3504. [PubMed: 22684783]

[129]. a) Kulkarni S, Feng S-S. Pharmaceutical Research. 2013; 30:2512–2522. [PubMed: 23314933] b) Soo Choi H, Liu W, Misra P, Tanaka E, Zimmer JP, Itty Ipe B, Bawendi MG, Frangioni JV. Nature Biotechnology. 2007; 25:1165–1170.

[130]. Vollrath A, Schallon A, Pietsch C, Schubert S, Nomoto T, Matsumoto Y, Kataoka K, Schubert US. Soft Matter. 2012; 9:99–108.

[131]. Hoffmann K, Behnke T, Grabolle M, Resch-Genger U. Anal Bioanal Chem. 2014; 406:3315–3322. [PubMed: 24429975]

[132]. Wang Z, Chen S, Lam JWY, Qin W, Kwok RTK, Xie N, Hu Q, Tang BZ. J Am Chem Soc. 2013; 135:8238–8245. [PubMed: 23668387]

[133]. Miki K, Kimura A, Oride K, Kuramochi Y, Matsuoka H, Harada H, Hiraoka M, Ohe K. Angewandte Chemie -International Edition. 2011; 50:6567–6570. [PubMed: 21656616]

[134]. Cho J, Kushiro K, Teramura Y, Takai M. Biomacromolecules. 2014; 15:2012–2018. [PubMed: 24761752]

[135]. Tong R, Coyle VJ, Tang L, Barger AM, Fan TM, Cheng J. Microscopy Research and Technique. 2010; 73:901–909. [PubMed: 20146347]

[136]. Yu Y, Feng C, Hong Y, Liu J, Chen S, Ng KM, Luo KQ, Tang BZ. Adv Mater. 2011; 23:3298–3302. [PubMed: 21671445]

[137]. Coelho M, Maghelli N, Tolic-Norrelykke IM. Integrative Biology. 2013; 5:748–758. [PubMed: 23525260]

[138]. a) Tyagi S. Nat Methods. 2009; 6:331–338. [PubMed: 19404252] b) Zhang J, Fei J, Leslie BJ, Han KY, Kuhlman TE, Ha T. Sci Rep. 2015; 5:17295. [PubMed: 26612428] c) Golding I, Cox EC. P Natl Acad Sci USA. 2004; 101:11310–11315.

[139]. a) Hicks BW, Angelides KJ. J Membr Biol. 1995; 144:231–244. [PubMed: 7658460] b) Saxton MJ, Jacobson K. Annual Review of Biophysics and Biomolecular Structure. 1997; 26:373–399.

[140]. Yu J, Wu C, Sahu SP, Fernando LP, Szymanski C, McNeill J. J Am Chem Soc. 2009; 131:18410–18414. [PubMed: 20028148]

[141]. Mascalchi P, Haanappel E, Carayon K, Mazeres S, Salome L. Soft Matter. 2012; 8:4462–4470.

[142]. Schädlich A, Rose C, Kuntsche J, Caysa H, Mueller T, Göpferich A, Mäder K. Pharmaceutical Research. 2011; 28:1995–2007. [PubMed: 21523513]

[143]. Schädlich A, Caysa H, Mueller T, Tenambergen F, Rose C, Göpferich A, Kuntsche J, Mäder K. ACS nano. 2011; 5:8710–8720. [PubMed: 21970766]

[144]. Zheng C, Zheng M, Gong P, Jia D, Zhang P, Shi B, Sheng Z, Ma Y, Cai L. Biomaterials. 2012; 33:5603–5609. [PubMed: 22575835]

[145]. a) Chaney EJ, Tang L, Tong R, Cheng J, Boppart SA. Molecular Imaging. 2010; 9:153–162. [PubMed: 20487681] b) Singh A, Lim C-K, Lee Y-D, Maeng J-h, Lee S, Koh J, Kim S. ACS Appl Mater Interfaces. 2013; 5:8881–8888. [PubMed: 23731221]

[146]. Yang Y, Song X, Yao Y, Wu H, Liu J, Zhao Y, Tan M, Yang Q. Journal of Materials Chemistry B. 2015; 3:4671–4678.

[147]. a) Panyam J, Labhasetwar V. Advanced Drug Delivery Reviews. 2003; 55:329–347. [PubMed: 12628320] b) Kumari A, Yadav SK, Yadav SC. Colloids and Surfaces B: Biointerfaces. 2010; 75:1–18. [PubMed: 19782542] c) Nicolas J, Mura S, Brambilla D, Mackiewicz N, Couvreur P. Chemical Society Reviews. 2013; 42:1147–1235. [PubMed: 23238558] d) Krasia-Christoforou T, Georgiou TK. Journal of Materials Chemistry B. 2013; 1:3002–3025.

[148]. Gustafson TP, Lim YH, Flores JA, Heo GS, Zhang FW, Zhang SY, Samarajeewa S, Raymond JE, Wooley KL. Langmuir. 2014; 30:631–641. [PubMed: 24392760]

[149]. Napp J, Behnke T, Fischer L, Würth C, Wottawa M, Katschinski DM, Alves F, Resch-Genger U, Schäferling M. Analytical Chemistry. 2011; 83:9039–9046. [PubMed: 22007722]

[150]. a) Gota C, Okabe K, Funatsu T, Harada Y, Uchiyama S. J Am Chem Soc. 2009; 131:2766–2767. [PubMed: 19199610] b) Ye F, Wu C, Jin Y, Chan Y-H, Zhang X, Chiu DT. J Am Chem Soc. 2011; 133:8146–8149. [PubMed: 21548583]

[151]. Peng, H-s, Stolwijk, JA., Sun, L-N., Wegener, J., Wolfbeis, OS. Angew Chem Int Ed. 2010; 49:4246–4249.

[152]. Yuan YY, Feng GX, Qin W, Tang BZ, Liu B. Chem Commun. 2014; 50:8757–8760.

[153]. Yuan YY, Zhang CJ, Liu B. Angewandte Chemie-International Edition. 2015; 54:11419–11423. [PubMed: 26094980]

Europe PMC Funders Author Manuscripts

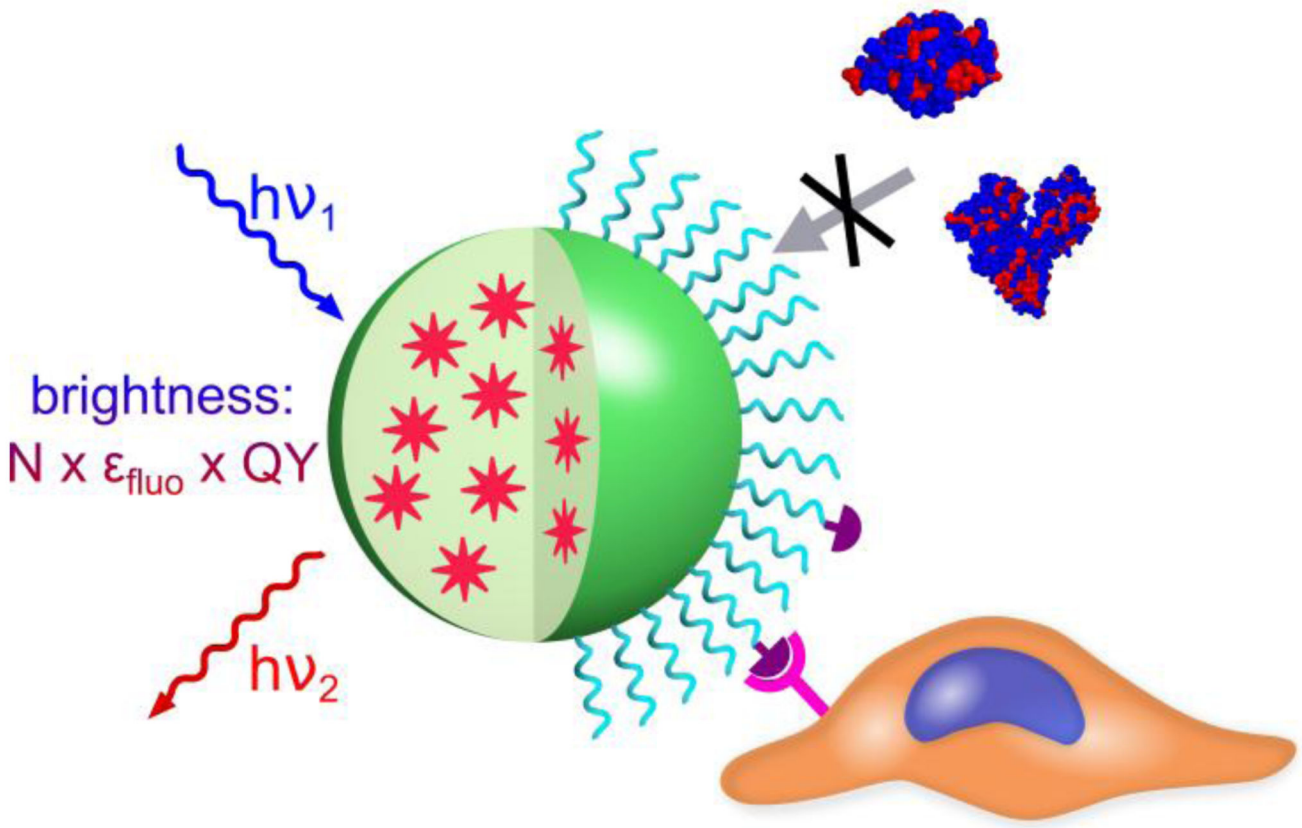

Figure 1.
Schematic view of dye-loaded polymer NP and the principal characteristics: brightness (proportional to number of encapsulated dyes, their extinction coefficient and quantum yield), control of non-specific interactions and implementation of selectivity.

Europe PMC Funders Author Manuscripts

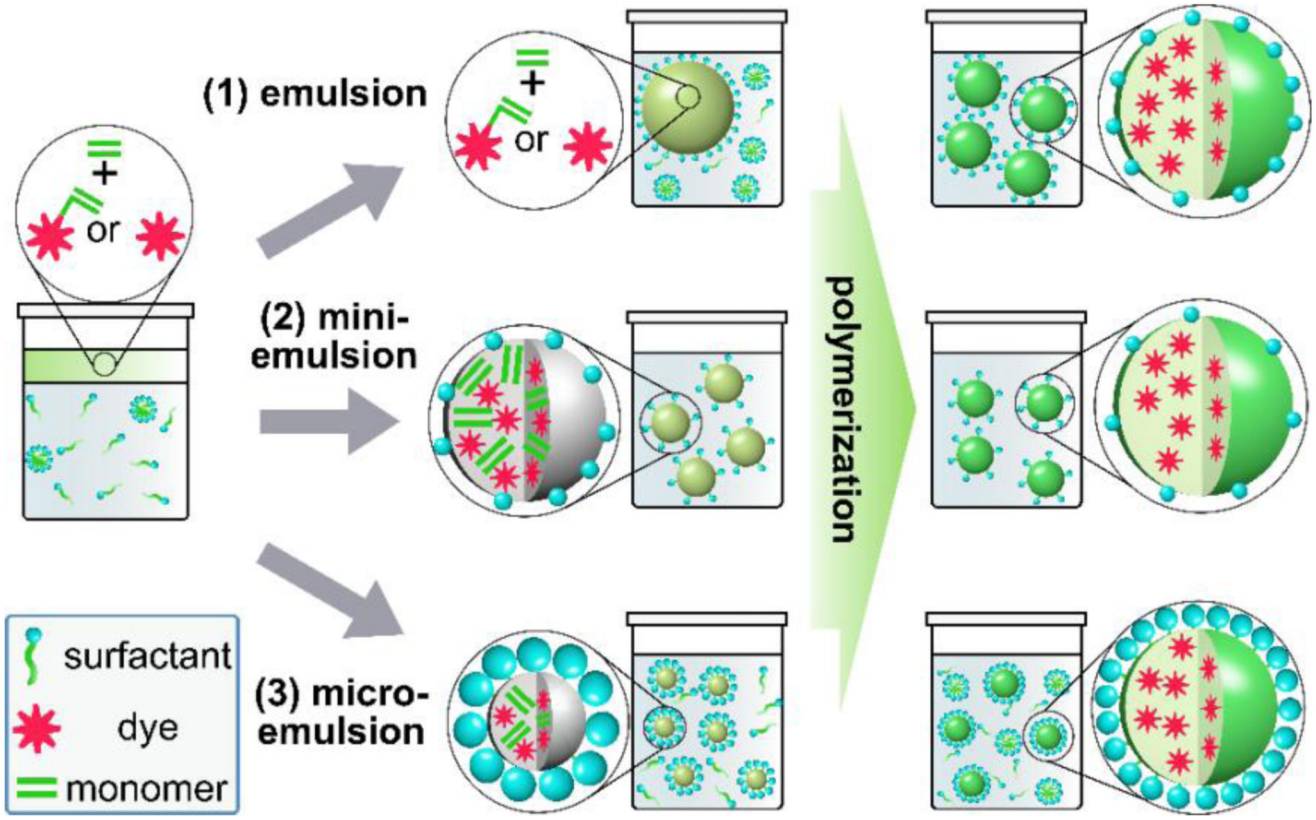

Figure 2.

Preparation of dye-loaded polymer NPs through conventional emulsion, mini-emulsion, or micro-emulsion polymerization. The type of emulsion formed depends on the concentration of the surfactant (> cmc in emulsion, < cmc in mini-emulsion, >> cmc in micro-emulsion) and the method of homogenization (shear in emulsion, high shear, ultrasound in mini-emulsion, low shear in micro-emulsion).

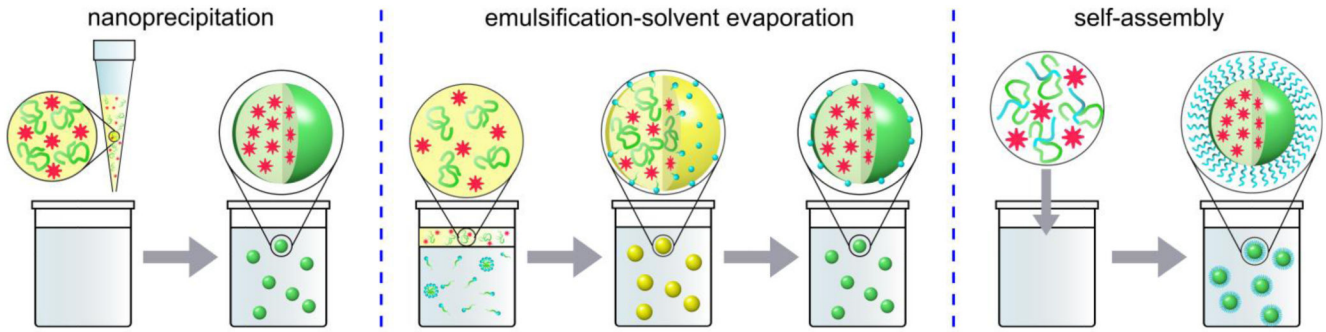

Figure 3.

Techniques used for the preparation of dye loaded NPs from preformed polymers. Hydrophobic polymer segments are shown in green, hydrophilic ones in blue, organic solvent in yellow.

Europe PMC Funders Author Manuscripts

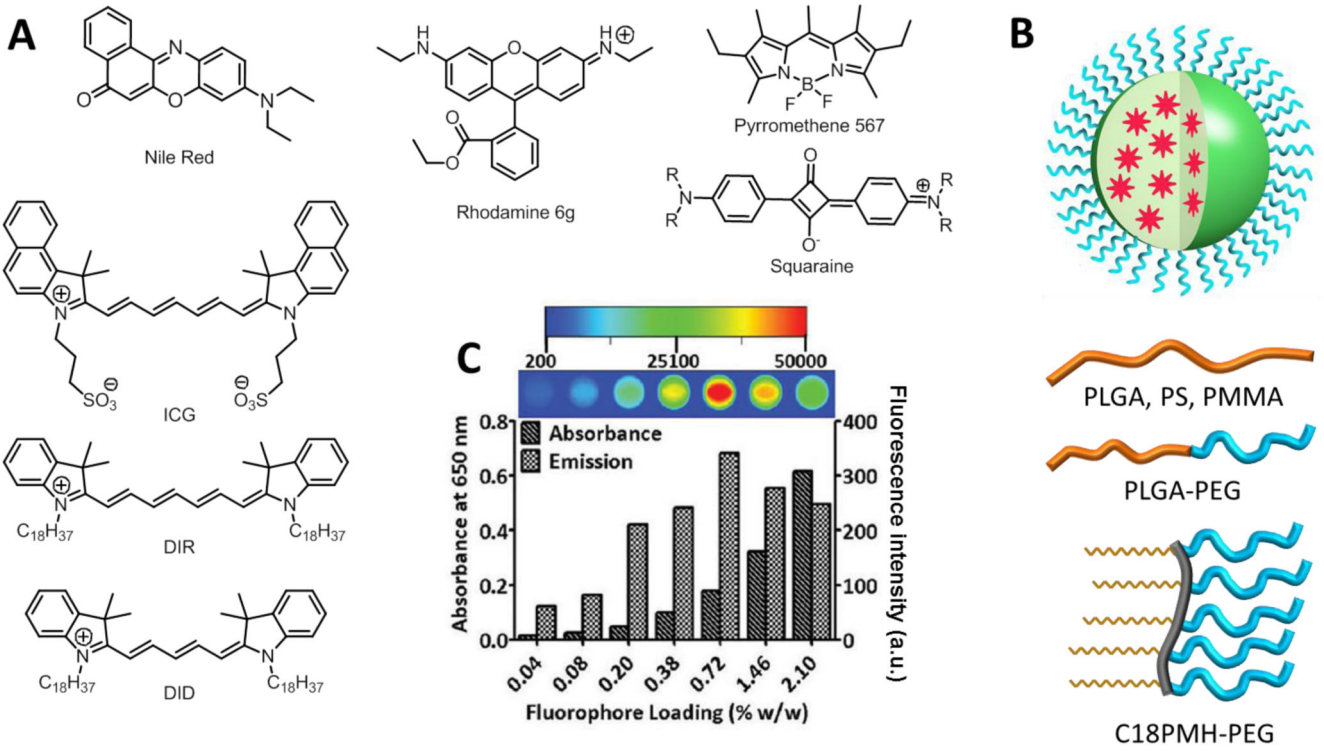

Figure 4.

(A) Conventional fluorescent dyes used for encapsulation into different types of polymer NPs. (B) Dye-loaded NP and its polymer constituents. (C) A bar chart showing the absorbance and fluorescence emission of DID-loaded PLGA-PEG nanoparticles (0.0−2.10% w/w). All samples consisted of the same number of particles (1×10^{11} particles) in deionized water (100 μL). Insets: The fluorescence images of the particles in a 96-well plate were acquired by a NIRF reflectance imaging system. Reprinted with permission.[57] Copyright 2012 American Chemical Society.

Europe PMC Funders Author Manuscripts

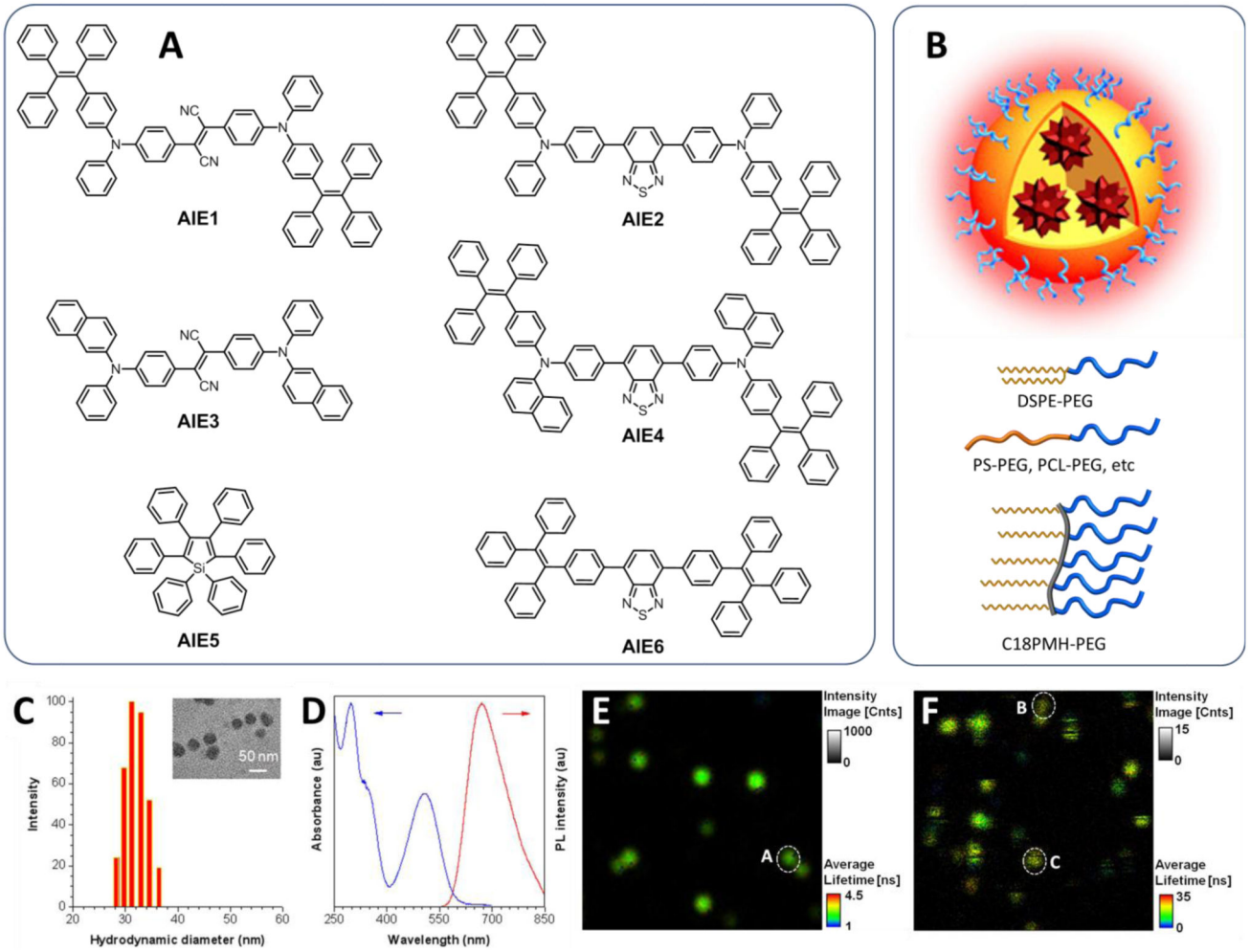

Figure 5.

(A) AIE dyes used for encapsulation into different types of polymer NPs. (B) AIE NP and surface active agents used to coat their surface. (C) Particle size distribution and morphological structure of Tat-AIE dots studied by laser light scattering (LLS) and (inset) high-resolution transmission electron microscopy (HR-TEM). (D) UV−vis absorption (blue) and PL (red) spectra of AIE1 NPs in water. (E, F) Fluorescence Lifetime Imaging of (E) Tat-AIE1 dots and Qtracker655 (E). The images were acquired upon excitation with a pulsed laser at 467 nm with a long-pass filter above 505 nm. The image is modulated by the pixel intensity (total photon counts) and the false color scale corresponds to the fluorescence lifetime value at each pixel of the image. Panels C-F were adapted with permission from Nature Publishing Group.[59a]

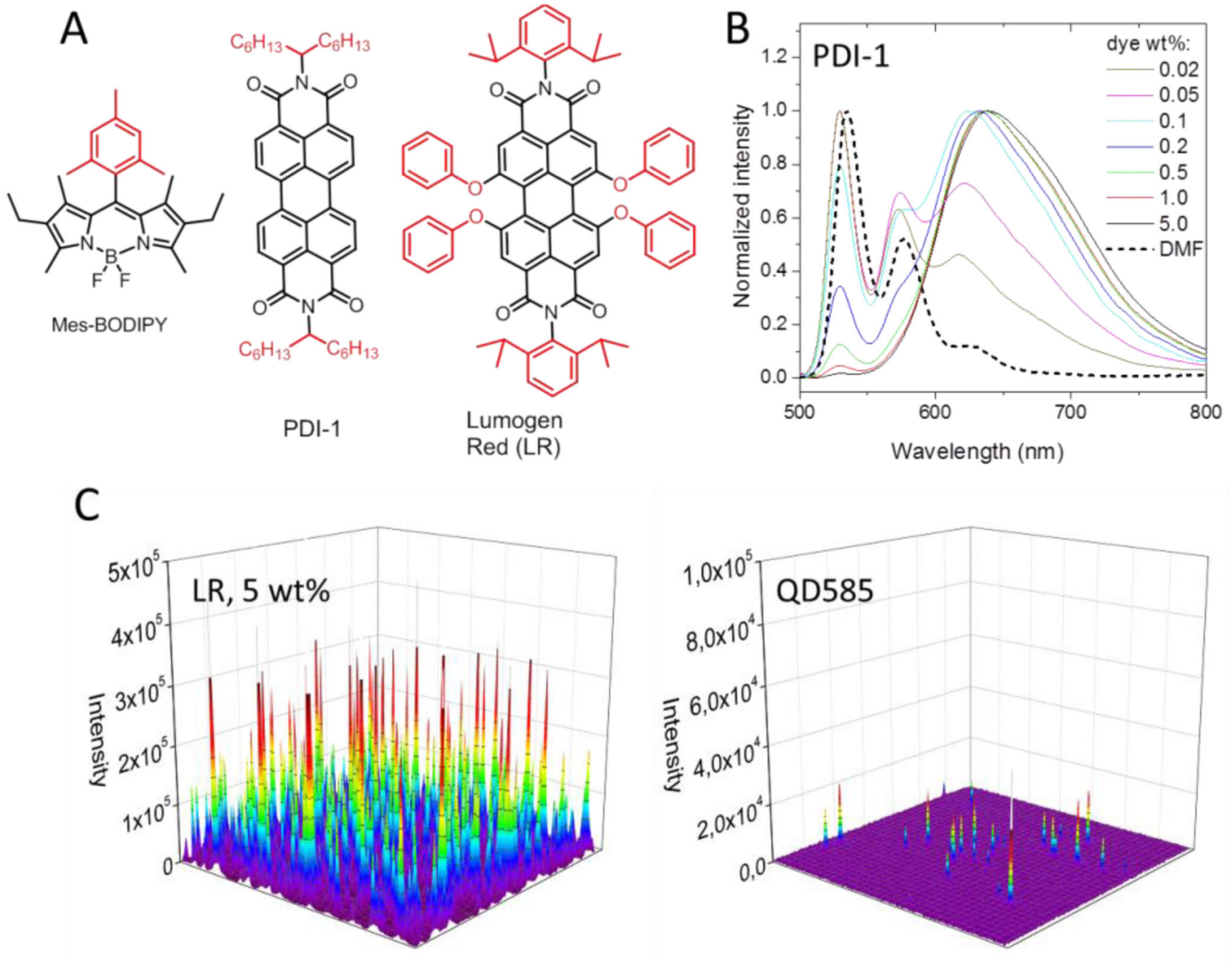

Figure 6.

Dyes bearing bulky groups used for encapsulation into polymer NPs and example of their properties. (A) Bulky groups are marked in red. (B) Emission spectra of 45 nm PLGA NPs loaded with different weight concentrations of PDI-1 (excitation at 485 nm). (C) Wide-field fluorescence microscopy images of fluorescent nanoparticles, encapsulating 5 wt% of LR on glass surface in comparison to QDs-585 under the same instrumental conditions. Illumination power was 5 W/cm^2 at 535 nm. Adapted from[22c] with permission from The Royal Society of Chemistry.

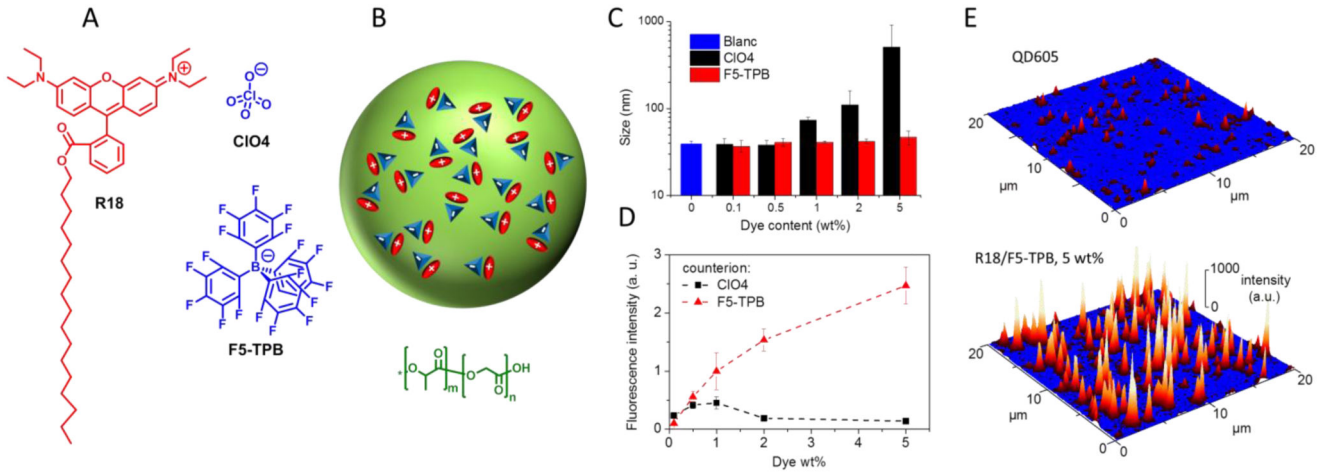

Figure 7.

Design and properties of dye-loaded polymer NPs using bulky counterions. (A) Chemical structures of rhodamine B octadecyl ester (R18) and its different counterions: perchlorate (ClO4), and tetrakis(pentafluorophenyl)borate (F5-TPB). (B) Schematic representation of PLGA NPs loaded with these dye salts. Size measured by DLS (C) and fluorescence intensity (D) of PLGA NPs *vs* dye content of R18 with different counterions. (E) Fluorescence microscopy images of quantum dots (QD605 streptavidin conjugate) and NPs containing 5 wt% of F5-TPB. The brightness of single QDs and PLGA NPs was 23 (±7) and 140 (±9), respectively. Micrographs were obtained under the same conditions of illumination and recording. Adapted with permission from from Nature Publishing Group.[23]

Europe PMC Funders Author Manuscripts

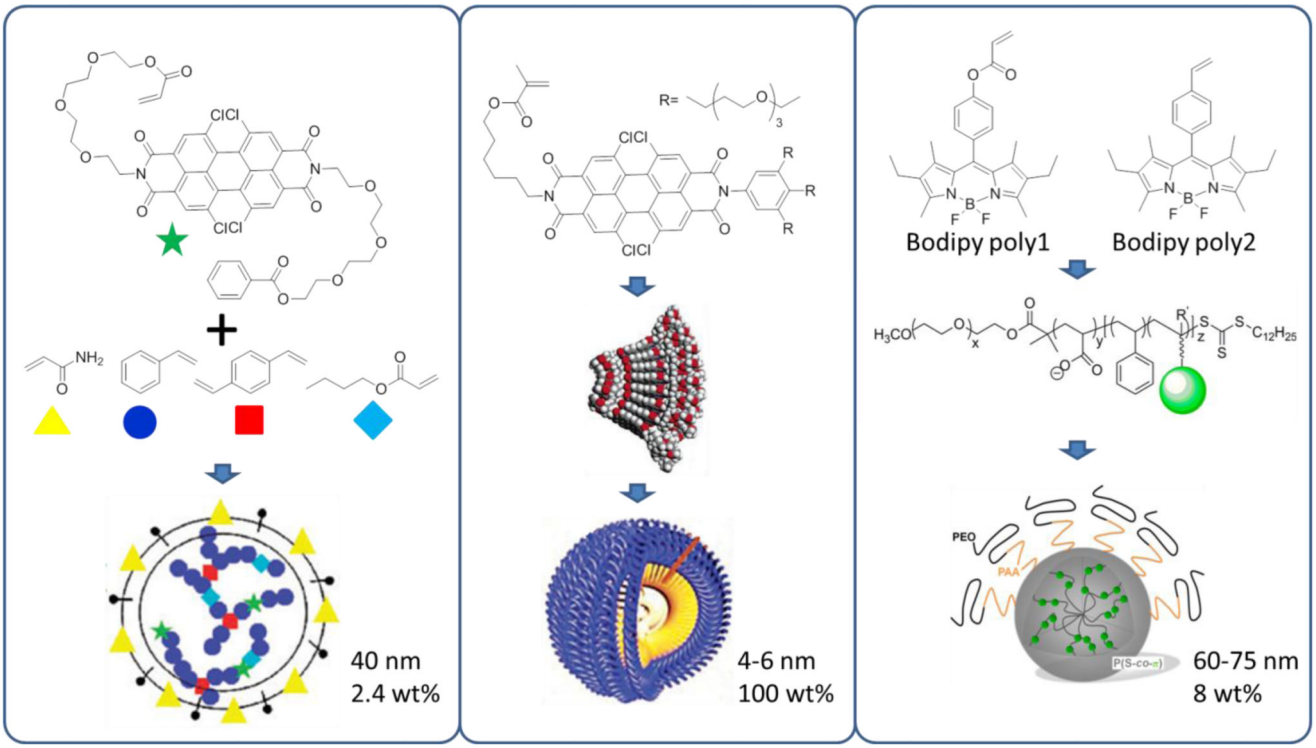

Figure 8.

Fluorescent monomers and their application for covalent encapsulation into different types of polymer NPs. Panels A adapted from[22b] with permission from The Royal Society of Chemistry. Panel B adapted with permission from.[95] Copyright 2007 American Chemical Society. Panel C adapted with permission from.[96] Copyright 2013 American Chemical Society.

Europe PMC Funders Author Manuscripts

Europe PMC Funders Author Manuscripts

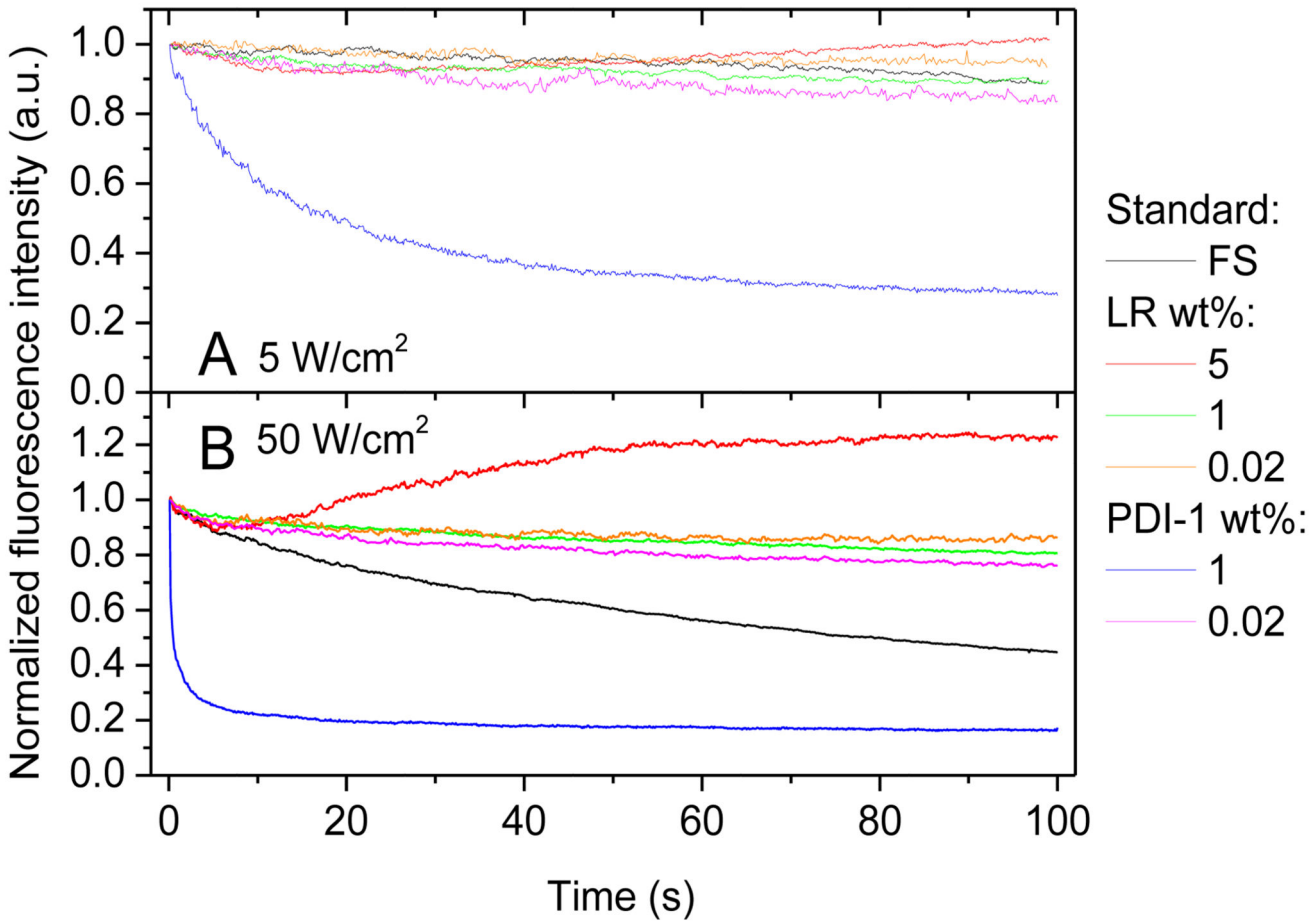

Figure 9.

Photostability of 45 nm PLGA NPs loaded with different amount of perylene diimide dyes PDI-1 and LR, measured by wide-field microscopy. NPs were immobilized on the glass surface and were continuously irradiated by a laser 532 nm at 5 (A) and 50 (B) W/cm^2. As a reference, FluoroSpheres (FS, FluoSpheres® Carboxylate-Modified Microspheres, 40 nm, red-orange fluorescent (565/580)) were used. Adapted from[22c] with permission from The Royal Society of Chemistry.

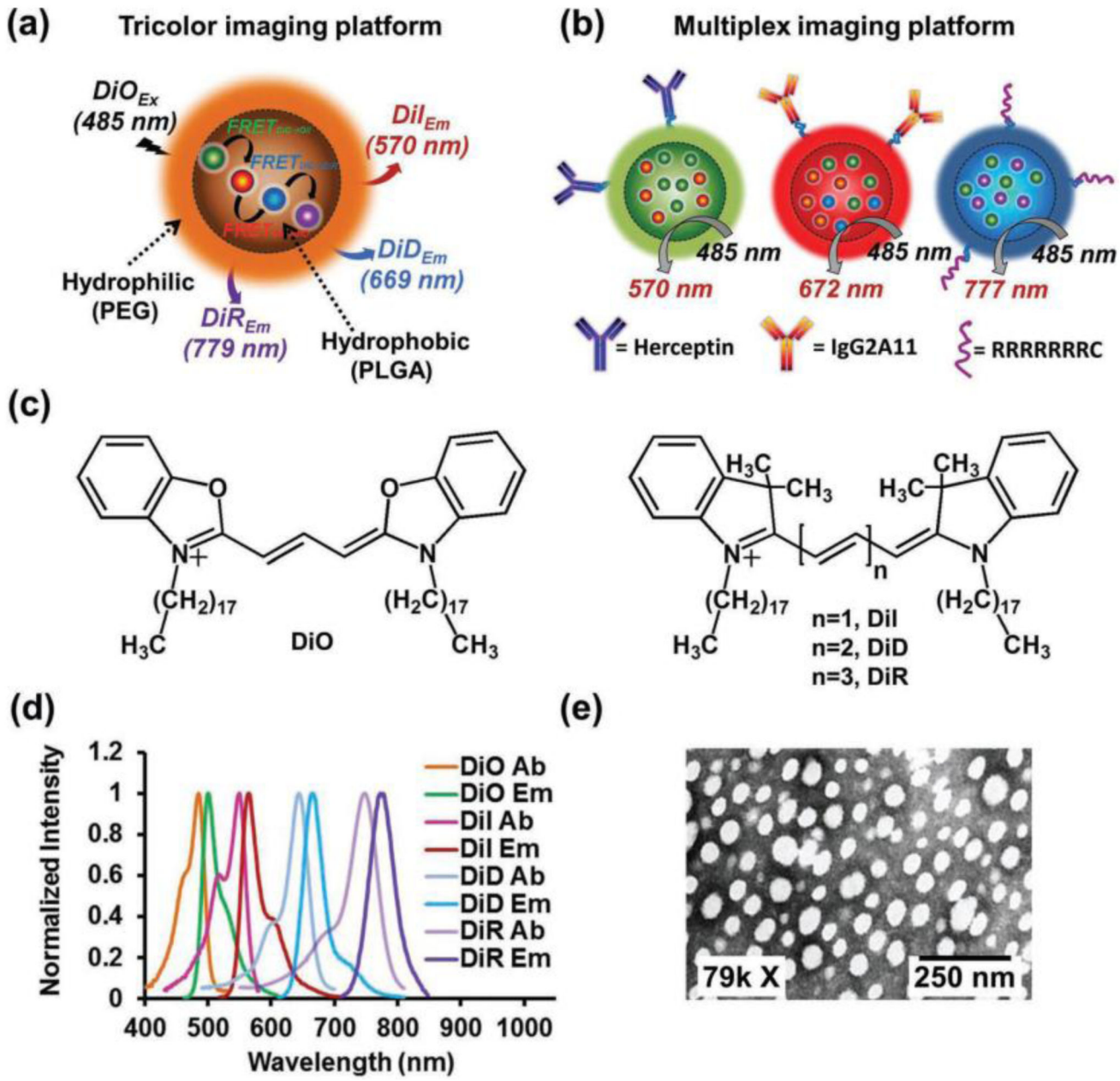

Figure 10.

A schematic representation of particles designed for (a) multicolor and (b) multiplex imaging. (c) The chemical structures of cyanine dyes DiO, DiI, DiD, and DiR. (d) A comparison of the normalized absorption and fluorescence emission spectra among the fluorophores in methanol. (e) A TEM image of the NPs. The samples were negatively stained with 2% (w/v) uranyl acetate in deionized water. Reproduced with permission from. [79] Copyright 2013 WILEY-VCH Verlag GmbH & Co.

Europe PMC Funders Author Manuscripts

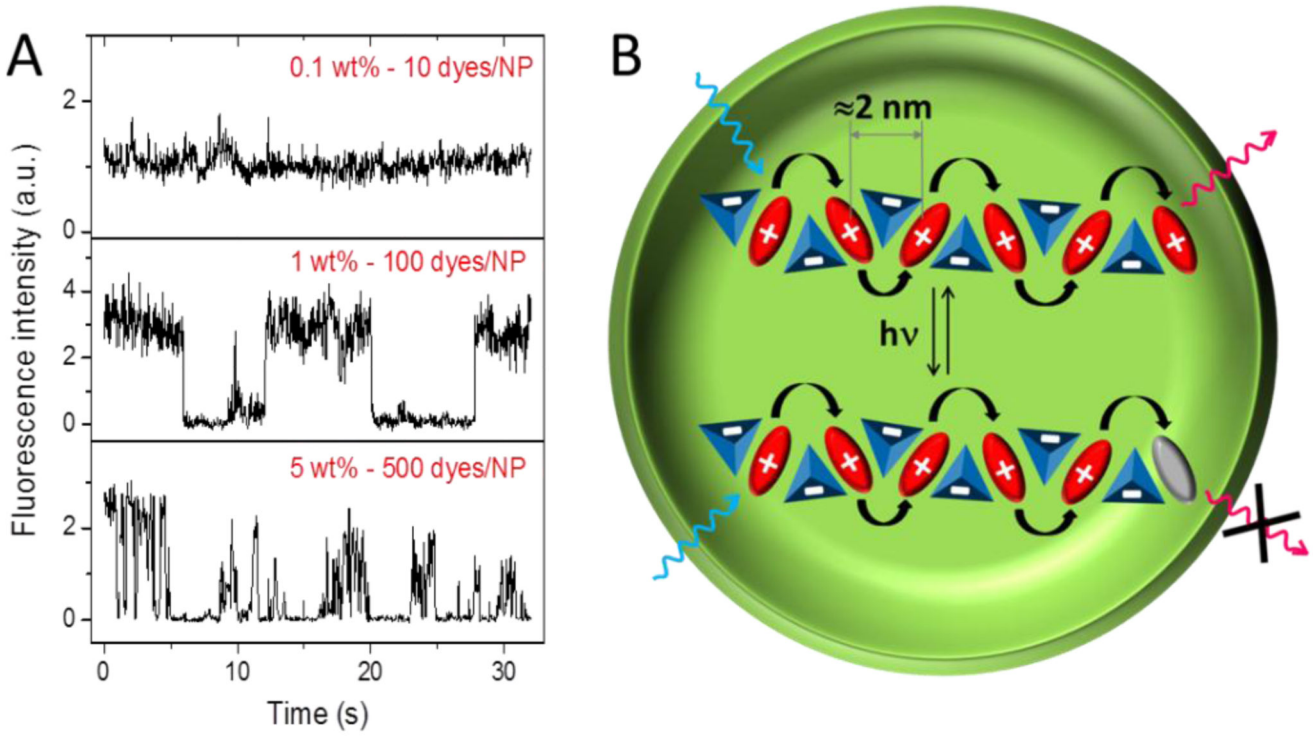

Figure 11.

Fluorescence on/off switching of dye-loaded NPs and proposed mechanism of blinking. (A) Emission transients of NPs, with 32-ms time resolution. Dependence of emission transients on R18/F5-TPB concentration. At least 200 particles per condition were analysed for the emission transients. The error bars correspond to s.e.m. (B) Short-range ordering (shown as 1D for simplicity) of R18 cations (red) by the F5-TPB counterion (blue) inside the polymer matrix (green) prevents dye aggregation and leads to the short inter-fluorophore distance suggested by the ultrafast EET. Dark species (grey) generated by light turn off the whole ensemble of dyes coupled by EET leading to on/off switching. Adapted with permission from from Nature Publishing Group.[23]

Europe PMC Funders Author Manuscripts

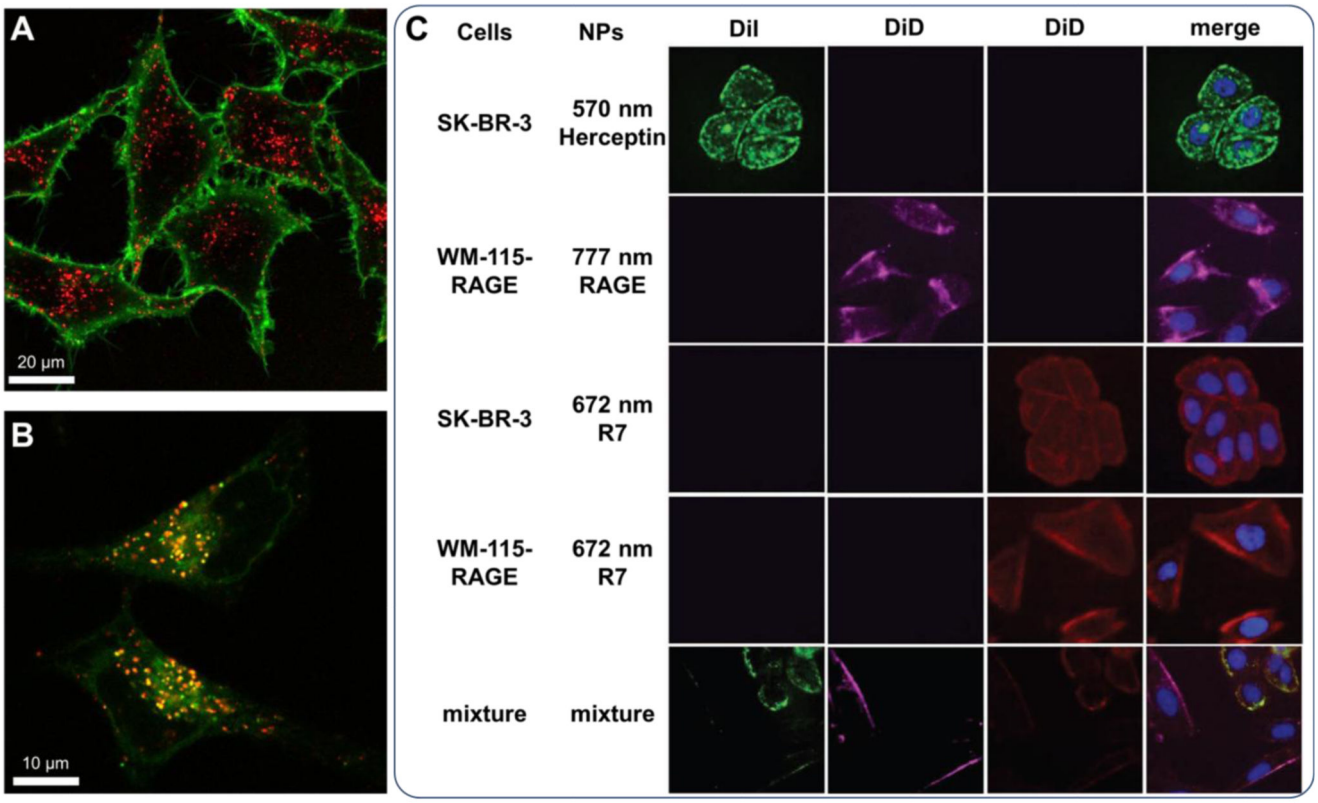

Figure 12.

Cellular imaging with dye-loaded NPs. (A) and (B) Confocal images of HeLa cells cultured for 3 h in the presence of PLGA NPs loaded with Rhodamine B octadecyl ester and a hydrophobic counterion (F5-TPB). (A) The membrane of the cells was labeled with wheat-germ agglutinin-Alexa488. (B) Incubation with LysoTracker Green DND-26 in order to label lysosomes. Adapted with permission from from Nature Publishing Group.[23] (C) Multiplexed imaging using the particles from Fig. 10. NPs emitting at 570, 777, and 672 nm and bearing, respectively, antibodies against (HER2) Herceptin and RAGE (IgG2A11), or a non-specific peptide (R7), were incubated with cells expressing HER2 (SK-BR-3) or RAGE (WM-115-RAGE) or mixtures thereof. All the cells were exposed to the same number of particles (9×10^{11} /mL, 400 μL) for 15 min at 37 °C. Hoechst 33342 (blue) was employed as the nuclear staining. The FRET images were acquired with the same excitation wavelength at 485 nm. Original magnification, 20X. Adapted with permission from.[79] Copyright 2013 WILEY-VCH Verlag GmbH & Co.

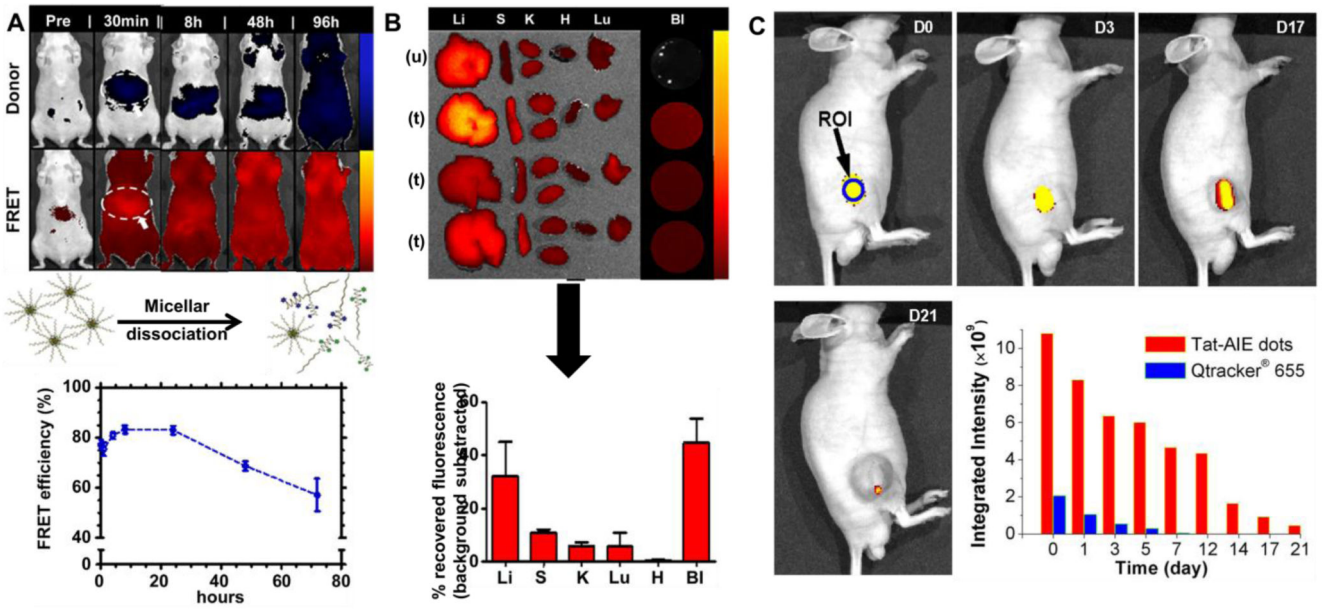

Figure 13.

In vivo imaging and cell tracking with dye-loaded NPs. (A-B) Imaging of copolymer micelles covalently labeled with Cy5 and Cy7 for FRET imaging. (A) Biodistribution of micelles using IVIS imaging. Top row corresponds to the donor fluorescent channel, λ_{ex} = 640 nm, λ_{em} = 700 nm; bottom row corresponds to FRET fluorescent channel, λ_{ex} = 640 nm, λ_{em} = 800 nm. Liver association is identified (circle and arrow). Bottom: FRET efficiency of micelles in circulation as a function of time (determined from live-animal bleeds following systemic administration). (B) Biodistribution after 24 h (n = 3). Images correspond to the FRET channel. Liver (Li), Spleen (S), Kidneys (K), Heart (H), Lungs (Lu), and Blood (Bl) extracted for each FRET micelle treatment and an untreated control for autofluorescence background. Bottom: quantification of recovered fluorescence. Adapted from, [94d] Copyright 2014, with permission from Elsevier. (C) *In vivo* fluorescence imaging of a mouse subcutaneously injected with 1×10^6 of C6 glioma cells after staining by 2 nM AIE loaded NPs. The inset shows the integrated PL intensities of the region of interest (ROI, blue circle) at the tumor site from the corresponding images and comparison to labeling with quantum dots Qtracker 655 used for labeling. Adapted with permission from Nature Publishing Group.[59a]

Table 1

Examples of dye-loaded NPs prepared by polymerization

Monomers	Surfactant (concentration)	Dye (concentration)	Homogenization	Size (nm)	Ref.
Conventional emulsion polymerization					
Sty, AA (95:5)	SDBS (1.5 mM)	PhE poly (AIE) (5%)	stirring	200	[32a]
MMA, HEMA, GMA (7:2:1)	SDS (8 mM)	Rhodamine 6G (0.4%)	stirring	40	[37]
Sty, DVB, VBAH	-	Fluorescein poly (3 mol%)	stirring	200, 500	[34b]
Mini-emulsion polymerization					
Sty, AA	SDS (8 mM)	PMI (0.05%)	sonication[a]	110	[38]
Sty	SDS (8 mM)	Bodipy surfmer (0.15%)	sonication[a]	100	[39]
Sty	PEG-PAA macro RAFT	Bodipy poly 2 (6.7%)	sonication	63	[40]
Micro-emulsion polymerization					
Sty, DVB	DTAB (0.5 M)	Pyr567 (0.5%), Bodipy (3.5%)[b]	Stirring	16 -30	[22a, 41]
AM	DOSS, Brij	Cyanines (1.5 wt%)	Stirring	28	[42]

a) Hexadecane (4 wt% rel mono)

b) through swelling or surface modification

Sty: styrene; AA: acrylic acid; MMA: methylmethacrylate; SDBS: sodium dodecyl benzene sulfonate; SDS: sodium dodecyl sulfate; PAA: polyacrylic acid; VBAH: vinylbenzylamine hydrochloride; DVB: Divinylbenzene; HEMA: hydroxymethylmethacrylate; PMI: *N*-(2,6-diisopropylphenyl)perylene-3,4-dicarbonacidimide Pyr567: Pyromethene 567; GMA: glycidyl methacrylate; DTAB: Dodecyltrimethylammonium bromide; AM: acrylamide; DOSS: Dioctyl sulfosuccinate; poly: polymerizable dye.

Europe PMC Funders Author Manuscripts

Table 2

Examples of dye loaded NPs prepared from preformed polymers

Polymer	Solvent	Homogenization	Dye (wt%)	Size (nm)	Ref.
		Emulsification solvent evaporation			
PLGA, PLGA-PEG[a]	CH_2Cl_2	sonication	AIE1 (10%)	180-210	[49]
Eudragit E[b]	CH_2Cl_2	sonication	NDA, Nile red (2.5%)	190-210	[50b]
		Nanoprecipitation			
PLGA	acetonitrile	stirring	Rhodamine B (5%)	40	[22c, 23]
PLGA-PEG	DMSO	-	DiD, DiR (2%)	50-80	[57]
P(MMA-co-MAS) (98.5:1.5)	acetonitrile	stirring	Rhodamine B (5%)	15	[54b]
DSPE-PEG	THF	sonication	Different AIE (30%)	30-80	[59a, 69]
C18PMH	THF	sonication	Squaraine (0.5%)	16	[70]
		Self-assembly			
PMAA-b-PS, PEG-b-PCL, PEG-b-PS	THF	stirring	AIE5 (20%)	63-85	[62b]
PEG-b-PVBA	DMF	Stirring	Fluorescein, Cy7, HL800	25	[62a]
HPMA, MATMA, TFMA copolymer	DMSO	Stirring	AIE dye (4-40%)	7-25	[64a]

[a] PVA (0.25, 2.5 %w/v)

[b] PVA (0.3-3 %w/v); NDA: naphthalene-2,3-dicarboxaldehyde; MAS: methacrylate ethylsulfonate; HPMA: N-(2-hydroxypropyl) methacrylamide; MATMA: [2-(methacryloyloxy)ethyl]trimethylammonium chloride; TFMA: 2,2,2-trifluoroethyl methacrylate; PVBA: poly(4-vinyl benzaldehyde).

Table 3

Examples of dye-based polymer NPs and their characteristics. Typical examples of conjugated polymers and quantum dots are given for comparison.

Dye	Polymer	Size (nm)	Dye content (wt%)	λ_{abs} (nm)	λ_{em} (nm)	QY (%)	B_T *(a)* ($M^{-1}cm^{-1}$)	B_E *(b)*	B/V ($M^{-1}m^{-1}nm^{-3}$)	Ref.
Molecular organic dyes										
Rh-101	-	1	100	565	588	90	9×10^4		166000	[103]
Quantum dots										
QD-605	-	11		*(c)*	605	55	3.2×10^5	-	458	
QD-585	-	8		*(c)*	585	60	1.8×10^5	-	680	
Conjugated polymer NPs										
PFBT	PFBT	10	100	460	540	30	3×10^6	30x QD-565	5700	[107]
MEH-PPV	MEH-PPV	15	100	485	590	1	2.6×10^6		1500	[17a]
MEH-PPV	MEH-PPV	74	90	485	593	1	1.4×10^8	-	665	[108]
MEH-PPV	MEH-PPV, PEG	3.33	-	496	593	1	1×10^4	-	511	[109]
Polymer NPs loaded with										
conventional dyes										
Nile red	PS	100	0.7	570	635	23	7×10^7	-	134	[75]
DiD	PLGA	66	0.5	650	667	21	1.3×10^7	-	84	[57]
Fluorescein	PS-b-PEG	24	0.5	495	519	22	5.1×10^5	-	120	[62a]
dyes bearing bulky side groups										
LR	PLGA	38	5	575	605	50	7.5×10^6	18x QD-585	261	[22c]
Mes-BODIPY	PS	16	3.5	526	540	77	5.1×10^6	-	2300	[22a]
aggregation induced emission dyes										
AIE6	DSPE-PEG	32	33	423	539	58	3.5×10^7	10x QD-655	1200	[59a]
AIE5	PS-b-PMAA	67	20	365	486	62	1.7×10^8	-	1000	[62b]
dyes with bulky counterions										
Rhodamine B/F5-TPB	PLGA	40	5	560	580	20	1.8×10^7	6x QD-605	600	[23]
Rhodamine B/F5-TPB	P(MMA-co-MAS)	15	5	560	580	60	3.0×10^6	10x QD-585	1600	[54b]
polymerizable dyes										
PDI (50,000)	PMMA	40	2.4	520	550	50	1.0×10^7	50-220x PDI	310	[22b]
BODIPY	PS-PEG	60	1.3	529	544	35	1.4×10^8	-	470	[96]

(a) BT is the theoretical and experimental brightness

(b) BE the experimental brightness.

(c) Calculated for excitation at 532 nm. Rh-101: rhodamine 101.

Europe PMC Funders Author Manuscripts

Table 4

Comparison of different fluorescent nanoparticles and organic dyes.[a]

	organic dyes	quantum dots	Conjugated polymer NPs	dye-loaded polymer NPs
Diameter[b]	~1 nm	6-60 nm	5-50 nm	15-100 nm
Monodispersity	+	+	+/-	+/-
Brightness (ε×QY)	10^3-10^5	10^5-10^6	10^5-10^8	10^5-10^8
Photostability[c]	10^5-10^6	10^7-10^8	10^6-10^9	4.4×10^7 [d]
Absorption range	UV-vis-NIR	UV-vis-NIR	UV-vis	UV-vis-NIR
Emission range	UV-vis-NIR	vis-NIR	UV-vis-NIR	UV-vis-NIR
Blinking	yes/no	Yes	yes/no	yes/no
Surface chemistry and colloidal stability	+	+	+/-	+/-
Biodegradability	+	-	-	+

[a] "+"– an advantage; "+/-" – to be improved; "-"– a weak point

[b] hydrodynamic diameter

[c] number of photons before photobleaching

[d] data from one report.[87]